

INFORMATION TO USERS

This dissertation was produced from a microfilm copy of the original document. While the most advanced technological means to photograph and reproduce this document have been used, the quality is heavily dependent upon the quality of the original submitted.

The following explanation of techniques is provided to help you understand markings or patterns which may appear on this reproduction.

1. The sign or "target" for pages apparently lacking from the document photographed is "Missing Page(s)". If it was possible to obtain the missing page(s) or section, they are spliced into the film along with adjacent pages. This may have necessitated cutting thru an image and duplicating adjacent pages to insure you complete continuity.
2. When an image on the film is obliterated with a large round black mark, it is an indication that the photographer suspected that the copy may have moved during exposure and thus cause a blurred image. You will find a good image of the page in the adjacent frame.
3. When a map, drawing or chart, etc., was part of the material being photographed the photographer followed a definite method in "sectioning" the material. It is customary to begin photoing at the upper left hand corner of a large sheet and to continue photoing from left to right in equal sections with a small overlap. If necessary, sectioning is continued again — beginning below the first row and continuing on until complete.
4. The majority of users indicate that the textual content is of greatest value, however, a somewhat higher quality reproduction could be made from "photographs" if essential to the understanding of the dissertation. Silver prints of "photographs" may be ordered at additional charge by writing the Order Department, giving the catalog number, title, author and specific pages you wish reproduced.

University Microfilms

300 North Zeeb Road
Ann Arbor, Michigan 48106
A Xerox Education Company

72-29,888

HEIMBACH, Jr., James Alvin, 1942-
A VARIATIONAL TECHNIQUE FOR MESOSCALE
OBJECTIVE ANALYSIS OF AIR POLLUTION.

The University of Oklahoma, Ph.D., 1972
Physics, meteorology

University Microfilms, A XEROX Company, Ann Arbor, Michigan

THE UNIVERSITY OF OKLAHOMA

GRADUATE COLLEGE

A VARIATIONAL TECHNIQUE FOR MESOSCALE OBJECTIVE
ANALYSIS OF AIR POLLUTION

A DISSERTATION

SUBMITTED TO THE GRADUATE FACULTY

in partial fulfillment of the requirements for the

degree of

DOCTOR OF PHILOSOPHY

BY

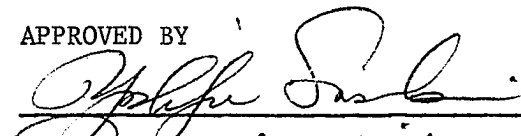
JAMES ALVIN HEIMBACH, JR.

Norman, Oklahoma

1972

A VARIATIONAL TECHNIQUE FOR MESOSCALE OBJECTIVE
ANALYSIS OF AIR POLLUTION

APPROVED BY



Raymond A. Miller

Frank J. Fontaine

John J. Gorman

DISSERTATION COMMITTEE

PLEASE NOTE:

Some pages may have

indistinct print.

Filmed as received.

University Microfilms, A Xerox Education Company

ABSTRACT

A variational technique has been developed which employs air quality monitoring data to obtain spatial estimates of contamination for a mesoscale area. A source inventory can be estimated from this technique which employs two or more contamination measurements and a reputable analytical diffusion model to best fit strengths to a system of strategically placed hypothetical sources as well as determine an optimal background contamination. At least two samples are needed because there is a minimum of two unknowns. The samples can be from the same time if they are not from the same location or as few as one per time period if the diffusion model reflects changing dispersion conditions. The solved parameters are applied in the same diffusion model to estimate the true contamination patterns with an optimal ensemble of plumes. A variational filter is then implemented to smooth the noisy portions of the analysis. The testing of the techniques on simulated data was satisfactory. Real SO₂ data were obtained from a survey of the Blackwell Zinc Company, Oklahoma, and use of these data gave realistic patterns.

ACKNOWLEDGMENTS

I am indebted to Dr. Yoshikazu Sasaki, Professor of Meteorology, for his advice and encouragement which he has freely given throughout our association. His thoughtful guidance has exposed me to many mathematical applications which were necessary for the completion of this project and which will be put to use in the future.

Dr. Rex Inman is gratefully recognized for his helpful scrutiny of my endeavors and his clarification of numerical procedures. He has presented me with many challenging problems from which I have gained much. Appreciation is extended to Drs. Raymond Mill, Carl Nau, and Frank Sonleitner, members of my Ph.D. committee who provided stimulation and consultation in this and other projects pursued while at the University of Oklahoma. Col. Frank Hall is acknowledged for his help with the synoptic analysis used in this study and Dr. Eugene Wilkins for our productive discussions of variational techniques applied to air pollution.

Mr. Kit Wagner and Mr. Charles Doswell, fellow students, deserve acknowledgment for the many fruitful discussions we had over the variational techniques applied in this study. Appreciation is extended to the Blackwell Zinc Company for permission to use their sulfur dioxide data and to Dr. Larry Canter and Mr. John Carter of the Department of Civil Engineering, the University of Oklahoma, who were responsible for the collection of this data. The assistance of Ms. Keven Amrein and Judy Virgiliowho typed the manuscript is appreciated.

Financial support for this study was provided through a traineeship sponsored by the National Science Foundation and the WEAT Program which is supported under the National Science Foundation Grant GA 30976. The National Center for Atmospheric Research, Boulder, Colorado, which is sponsored by the National Science Foundation, is acknowledged for use of the Control Data 6600 and 7600 computers.

I could not have carried out my graduate studies without the closeness and inspiration of Linda, my wife.

TABLE OF CONTENTS

	Page
ACKNOWLEDGMENTS.	iv
LIST OF TABLES	viii
LIST OF ILLUSTRATIONS.	ix
LIST OF SYMBOLS.	x
 Chapter	
I. INTRODUCTION.	1
Statement of Problem.	2
II. DIFFUSION MODELING: A REVIEW AND APPLICATION	4
Analytical Solutions to Diffusion Equation.	4
The Gaussian Plume Assumption	6
Other Modeling Techniques	7
An Application.	9
III. VARIATIONAL TECHNIQUE TO FIND OPTIMAL SOURCE AND BACKGROUND VALUES	12
Derivation of Analysis Equations.	12
Analysis of Input Error	14
IV. A VARIATIONAL LOW-PASS FILTER	16
Characteristics of the Filter	17
Numerical Solution to Low-Pass Analysis Equation.	20
V. AIR POLLUTION DATA.	22
VI. METEOROLOGICAL CONDITIONS FOR TWO TEST DAYS	25
August 11	25
August 17	25
Choice of Weather Parameters for Diffusion Estimation	26

	Page
VII. TESTING TECHNIQUES WITH REAL DATA	27
Preliminary Test Results.	28
One Location Out of Three Used as a Control	28
Two Locations Out of Three Used as Control Data	30
VIII. CASE STUDIES.	32
IX. CONCLUSIONS AND REMARKS	36
BIBLIOGRAPHY	38
Appendix	
A. A FUNDAMENTAL SOLUTION FOR FICKIAN DIFFUSION.	41
B. GAUSSIAN PLUME MODELING	43
C. DERIVATION OF EULER-LAGRANGE EQUATION FOR LOW-PASS FILTER.	47
D. CONVERGENCE OF LOW-PASS FILTER.	49

LIST OF TABLES

Table	Page
I. BLACKWELL AIR QUALITY CONTROL DATA FROM 11 AND 17 AUGUST, 1971	52
II. TESTING OPTIMIZATION USING A LARGE SAMPLE AS CONTROL IN SINGLE PERIOD ANALYSIS.	53
III. TESTING OPTIMIZATION USING A SMALL SAMPLE AS CONTROL IN SINGLE PERIOD ANALYSIS.	54
IV. TESTING OPTIMIZATION USING A MEDIUM SAMPLE AS CONTROL IN SINGLE PERIOD ANALYSIS.	55
V. RESULTS OF MULTIPLE PERIOD ANALYSIS USING ONE CONTROL SITE FOR 11 AUGUST, 1971	56
VI. RESULTS OF MULTIPLE PERIOD ANALYSIS USING ONE CONTROL SITE FOR 17 AUGUST, 1971	57
VII. SINGLE PERIOD AND MULTIPLE PERIOD ANALYSES FOR 11 AUGUST, 1971	58
VIII. SINGLE PERIOD AND MULTIPLE PERIOD ANALYSES FOR 17 AUGUST, 1971	59

LIST OF ILLUSTRATIONS

Figure	Page
1. Response of Filtered Mode.	60
2. Blackwell, Oklahoma.	61
3. Blackwell Zinc Company	62
4. Surface Situation of 0700 CDT, 11 August, 1971	63
5. Surface Situation of 1900 CDT, 11 August, 1971	64
6. Oklahoma City Soundings of 11 August, 1971	65
7. Surface Situation of 0700 CDT, 17 August, 1971	66
8. Surface Situation of 1900 CDT, 17 August, 1971	67
9. Oklahoma City Soundings of 17 August, 1971	68
10. Error of Single Period Analysis Testing.	69
11. Contoured Contamination for Single Period Test, One Control Site	70
12. Contoured Contamination for Multiple Period Test, One Control Site	71
13. Error of Multiple Period Analysis, One Control Site. . .	72
14. Same as 13, Two Control Sites.	73
15. Contoured Multiple Period Analysis, Two Control Sites. .	74
16. Contoured Single Period Analysis, Morning of 11 August, 1971	75
17. Same as 16, Afternoon of 11 August, 1971	76
18. Same as 16, Morning of 17 August, 1971	77
19. Same as 16, Afternoon of 17 August, 1971	78
20. Contoured Multiple Period Analysis, Morning of 11 August, 1971	79

Figure	Page
21. Same as 20, Morning of 11 August, 1971	80
22. Same as 20, Morning of 17 August, 1971	81
23. Same as 20, Afternoon of 17 August, 1971	82

LIST OF SYMBOLS

χ	concentration of air pollutant
K	eddy diffusivity
t	time
x, y, z	three directions of Cartesian coordinates
∇	dimensional differential operator ($\partial/\partial x, \partial/\partial y, \partial/\partial z$)
Q	source or "pseudo-source" strength
\bar{u}	mean wind velocity
σ	standard deviation (with x, y, z components σ_x, σ_y and σ_z in Cartesian coordinates)
v'	instantaneous wind velocity component crosswind to the direction of the mean flow
D	depth of the mixing layer of a specific pollutant
χ_b	background contamination
σ_θ	horizontal angular standard deviation of a Gaussian plume
F	relative concentration of contamination, χ/Q
w_y	a parameter of σ_y to account for crosswind size of a source
w_z	a parameter of σ_z to account for vertical size of a source
T	a factor used to account for the increased plume width as a function of sample averaging time
h	half life time of a contaminant
$\tilde{\chi}$	observed contamination
λ	an eigenvalue for an ordinary differential equation
$c_1, c_2, \left. \begin{matrix} c_3, c_4, c \end{matrix} \right\}$	constants of integration

i	an index referring to pseudo-source location
I	total number of pseudo-source locations
n	an index referring to sampling location
N	total number of sample locations
J	variational functional
δ	variational operator
γ_1, γ_2	relaxation factors
ϵ	random error
κ	curvature of analyzed contamination field
χ'	the first approximation of contamination field
α_1	nondimensional weight for observation of concentration, $\tilde{\chi}$
α_2	nondimensional weight for the first guess data, χ'
β_1	nondimensional weight for the smoothing term expressed by the gradient of contamination squared
β_2	nondimensional weight for the smoothing term expressed by the second gradient of contamination squared
∇_x	nondimensional differential operator, $\partial/\partial x$, in x-dimension
∇_{xy}	nondimensional differential operator in x and y-dimensions, $\partial^2/\partial x \partial y$
Ω	horizontal domain bounded by perimeter of mesh
∇_{xxyy}	nondimensional fourth order operation in two dimensions, $\partial^4/\partial x \partial x \partial y \partial y$
a	a parameter which is equal to $1/2\sigma y^2$
L	size of the domain Ω on the x-coordinate
a_i	the i th Fourier coefficient of cosine expansion for the true contamination pattern, $\tilde{\chi}$
A_i	same as a_i but for contamination pattern, χ
R_n	response function of the Euler equation for the n^{th} harmonic

ψ_{xx}	a second order nondimensional centered space finite difference operator in one direction
ψ_{xxyy}	a fourth order nondimensional centered space finite difference operator in two dimensions
p, q	empirical parameters used to estimate σ_y and σ_z , respectively, in Bosanquet-Pearson model
C_y, C_z	empirical parameters used to estimate σ_y and σ_z , respectively, in Sutton models
n_y, n_z	empirical parameters used to estimate σ_y and σ_z , respectively, in modified Sutton model
M_y, M_z	empirical parameters used to estimate σ_y and σ_z , respectively, in USPHS-TVA model
t'	time of release of a puff of smoke
$L[\]$	linear operator
$R^{(m)}$	residual of finite difference analogue of Euler equation at pass m
$\Delta\chi^{(m)}$	error in analyzed contamination at pass m
Δs	grid size
G	amplification factor
μ, η	wave number in the x and y directions, respectively

A VARIATIONAL TECHNIQUE FOR MESOSCALE OBJECTIVE ANALYSIS OF AIR POLLUTION

CHAPTER I

INTRODUCTION

Urban areas generally have very sparse air quality monitoring data, if any, except for the large scale air resource projects such as the study currently in process in St. Louis (Changnum, et al., 1971). An awareness of the biological, medical and economical problems of air pollution is dependent upon a sound analysis of the contamination situation. For example, the Nashville air pollution study (Zeidberg et al., 1964) used such data to demonstrate a positive correlation of morbidity with contamination as determined by a dense sampling network. Heimbach (1971), however, had to use estimates of climatological sulfur dioxide (SO_2) patterns for Altoona, Pa., as found by a pollution model, to show a correspondence between pollution and lung ailments as well as with botanical damage. For routine use of air pollution data in areas not having a dense sampling network, some valid technique should be developed to estimate true patterns of contamination from sparse air quality control data.

The interpolation of irregularly spaced data to a system of regularly spaced points is a topic in objective analysis. Few objective

analysis schemes have been applied in the field of air pollution. Mahoney, et al. (1970) performed a macroscale analysis for the New England area using the SYMAP and SYMVU programs which involve weighted interpolation schemes. The method gave reasonable patterns in areas of dense sampling, however, in areas of inadequate data input, the concentrations were unrealistically high.

Many models exist which estimate contamination patterns as a function of source strength and various meteorological parameters. A survey of these is presented in Chapter II. In many of these models the diffusion coefficients which appeared are difficult to determine in an urban area where vertical soundings are not made with sufficient frequency (hourly vertical soundings seem to be required). Also, these are dependent upon a source inventory which is difficult to determine accurately.

A very promising application has been proposed by Wilkins (1971) which uses the method of numerical variational analysis (Sasaki, 1958). Wilkins' technique would find an optimized pattern of contamination over an urban area which would best fit sampling data as well as comply with the dynamical constraints of advection and diffusion with source and sink terms included. Though a variational analysis was employed in this case, it is not the same as either of the variational techniques developed in Chapters III and IV.

Statement of Problem

Widespread air pollution episodes such as that of Thanksgiving, 1966 (Fensterstock and Fankhauser, 1968), involve pollutants transported over long distances or over international boundaries (Royal Ministry of

Foreign Affairs and Royal Ministry of Agriculture, 1971). Hall and Hagan (1971) have shown this to be the case in a subjective analysis of an episode which occurred in the central United States, August, 1970. Thus, a receptor location should be affected by distal sources which contribute the background contamination. Local sources, which account for peaks, are superimposed on the background concentration. An analysis technique should distinguish between the two if it is to be used routinely in planning, abatement and research.

The technique to be developed addresses itself to three questions: a) how can sparse air quality control data be used effectively to provide contamination patterns as a function of background and localized contributions, b) how is this to be done without utilizing a source inventory or without knowing the background contamination, and c) how can the concentrations due to local sources and distal sources, namely background contamination, be separated.

The methods developed in Chapters III and IV, and tested in Chapters VII and VIII, are an attempt to do this by using a variational approach to optimize a background contamination and a system of hypothetical source strengths or "pseudo-sources" which best fit the data and any applied diffusion model. An objective analysis is completed where the diffusion model incorporates these optimized parameters to obtain pollution values at the evenly spaced grid locations. A low-pass variational filter is then applied to smooth the noisy portions of the resulting pseudo-source plume ensemble.

CHAPTER II

DIFFUSION MODELING: A REVIEW AND APPLICATION

Analytical Solutions to Diffusion Equation

The prediction of atmospheric diffusion had its beginnings during World War I when it was necessary to understand the fate of smoke and poison gas (Ross, 1970). During this period there were many analytical solutions derived for simplified versions of the diffusion equation

$$\frac{d\chi}{dt} - \nabla \cdot K \nabla \chi + \text{source term} - \text{sink term} = 0 . \quad (2.1)$$

Haltiner and Martin (1957) and Sutton (1953) give a review of the solutions for various boundary and initial conditions. The first application was done by Bosanquet and Pearson in 1936 (Montgomery and Corn, 1967) and many more followed. The specifics of these models are listed in Appendix B.

For the case of Fickian diffusion where the mean wind is zero, (2.1) for one dimension is written:

$$\frac{\partial \chi}{\partial t} - K \frac{\partial^2 \chi}{\partial x^2} = 0 . \quad (2.2)$$

The general solution, as shown in Appendix A, is (Courant and Hilbert, 1962)

$$\chi = \frac{c}{t^{\frac{1}{2}}} \exp \left[\frac{-x^2}{4Kt} \right] , \quad (2.3)$$

The constant c can be determined for an instantaneous puff of smoke having the following conditions:

$$\chi \rightarrow 0 \quad \text{as} \quad t \rightarrow 0 \quad \text{for} \quad x \neq 0 ,$$

$$\chi \rightarrow 0 \quad \text{as} \quad x \rightarrow \pm\infty ,$$

and

$$\int_{-\infty}^{\infty} \chi \, dx = Q ,$$

and the solution is now given as:

$$\chi = \frac{Q}{2\sqrt{\pi t K}} \exp \left[-x^2/4Kt \right] . \quad (2.4)$$

This is easily extended to homogeneous diffusion in three dimensions (Roberts, 1923):

$$\chi = \frac{Q}{8(\pi K t)^{3/2}} \exp \left[-\frac{(x^2 + y^2 + z^2)}{4Kt} \right] . \quad (2.5)$$

For horizontal steady state conditions from a point source where advection far exceeds downwind diffusion, Eq. (2.1) is rewritten as

$$\bar{u} \frac{\partial \chi}{\partial x} - K \frac{\partial^2 \chi}{\partial y^2} = 0 . \quad (2.6)$$

Assuming the \bar{u} is constant, the basic solution of Eq. (2.6) for a point source at $x = 0$ is

$$\chi = \frac{c}{x^{1/2}} \exp \left[-\frac{\bar{u} y^2}{4Kx} \right] . \quad (2.7)$$

Applying the conditions

$$\chi \rightarrow 0 \quad \text{as} \quad y \rightarrow \pm\infty ,$$

$$\chi = 0 \quad \text{for} \quad x < 0 ,$$

and

$$\int_{-\infty}^{\infty} \bar{u} \chi \, dy = Q, \text{ a source rate ,}$$

the constant of (2.6) can be found:

$$\chi = \frac{Q}{2\sqrt{\pi Kx}} \exp \left[-\frac{\bar{u}y^2}{4Kx} \right] . \quad (2.8)$$

Extension into three dimensions assuming a homogeneous K gives

$$\chi = \frac{Q}{4\pi Kx} \exp \left[-\frac{\bar{u}(y^2 + z^2)}{4Kx} \right] . \quad (2.9)$$

The Gaussian Plume Assumption

The results (2.4) through (2.9), though derived analytically, can be compared to a binormal distribution in the vertical and cross-wind directions multiplied by a downwind stretching term, $1/\bar{u}$, which results from the assumption that $x = \bar{u}t$.

$$\chi = \frac{Q}{2\pi\sigma^2\bar{u}} \exp \left[-\frac{(y^2 + z^2)}{2\sigma^2} \right], \quad (2.10)$$

where σ represents the standard deviation of a homogeneous pollution concentration profile in the vertical and cross wind directions. One verification of this Gaussian configuration has been proven by Syono (1953) using random walk.

Eq. (2.10) is exactly equivalent to (2.9) if

$$\sigma = \sqrt{2Kx/\bar{u}} . \quad (2.11)$$

Isotropic turbulence is rarely the case, therefore

$$\chi = \frac{Q}{2\pi\sigma_y\sigma_z\bar{u}} \exp \left[-\frac{y^2}{2\sigma_y^2} - \frac{z^2}{2\sigma_z^2} \right] , \quad (2.12)$$

and the transform from the analytical solution to Eq. (2.12) is accomplished by setting

$$\sigma_y = \sqrt{2K_y x / \bar{u}}, \text{ and } \sigma_z = \sqrt{2K_z x / \bar{u}}. \quad (2.13)$$

The eddy diffusion coefficients, K 's, are very difficult to estimate. Rather, the practice has been to determine the standard deviations empirically using a tracer or some identifiable contaminant. This technique has given very satisfactory results in the mesoscale and the Gaussian plume models have therefore enjoyed a good measure of success. Taylor (1920), in the first statistical treatment of the diffusion problem, related a particle's standard deviation of crosswind distance, y , to the Lagrangian autocorrelation coefficient of the wind velocity component crosswind to the average wind direction (v').

$$\overline{y^2} = \sigma_y^2 = 2\overline{v'^2} \int_0^{t'} \int_0^t R(\xi) d\xi dt \quad (2.14)$$

This Lagrangian estimate of standard deviation can be used as an estimate of the spatial (Eulerian) standard deviation of many particles if the ergodic principal is valid (Munn, 1966). That is, when time averages for one particle are the same as space averages for many.

Other Modeling Techniques

Several other models have been applied with some success. More than a very brief mention of them is beyond the scope of this discussion. The simplest is the "box model" (Lettau, 1970) where an inventory of contamination input and output is used to estimate pollution concentrations within a box bounded by the surface, mixing height and width of concerned area. Transport is done through horizontal advection through the boundaries and instant vertical mixing.

The "top hat model" (Turner, 1969) is a simplified version of Eq. (2.12). Instead of a binormal distribution of concentration, the contami-

nants are assumed to have a constant density vertically throughout a mixing layer of depth D and horizontally on a downwind arc, usually $\pi/8$ radians.

$$\chi = \frac{8Q}{D\pi\bar{x}\bar{u}} \quad (2.15)$$

This model has given adequate results for long term averages and is much less cumbersome than (2.12).

There are several classes of statistical models which involve climatology and regression (Mahoney, 1970). The climatology approach is useful when there is no weather or source information available as for a long range pollution forecast. The generalized regression formulation is

$$\chi = \chi_b + \sum_{i=1}^1 \sum_{j=-m}^n a_{i,j} b^j, \quad (2.16)$$

where χ_b is background contamination, the b 's are predictors such as inversion height and dewpoint which are taken to the j th power and the a 's are regression coefficients. Because these models involve historical data, they are limited to predictions which assume no change in source configuration.

More recently, models involving numerical solutions of the diffusion equation (2.1) have been applied (see for example, Pandolfo et al., 1971; Egan and Mahoney, 1972). These involve some form of boundary layer model to predict or analyze the meteorological parameters. The greatest problem is to estimate the eddy diffusivities which are a function of space scales and averaging time as well as meteorological parameters determined by a boundary layer model. The initial conditions to these models have been to impose concentrations which are initially set to zero or to a homogeneous background level. A large enough period between initial and analysis or forecast time is assumed so that the error of such initial

conditions is damped out.

An Application

The variational analysis scheme described in Chapter III requires a diffusion estimate which is sensitive to downwind and crosswind distances from a source, wind velocity and stability. Two Gaussian plume models were chosen, the Pasquill-Gifford and the USPHS-TVA treatments (see Appendix B, Eqs. (B-7) and (B-9)) to test the sensitivity of the analysis technique to different diffusion models. The Pasquill-Gifford version tends to spread a plume laterally faster than the other for similar source and meteorological conditions.

There were some changes incorporated into the two models to account for volume sources and the long averaging times of the pollution data used. Sources which were other than a point had their horizontal and/or vertical size accounted for by the addition of a constant to the respective standard deviation of concentration profile. These constants, w_y and w_z , were the width and height of the source divided by 4.3 (Turner, 1969),

$$\begin{aligned}\sigma_y (\text{adjusted}) &= \sigma_y + w_y = \sigma_y + \text{width}/4.3, \\ \sigma_z (\text{adjusted}) &= \sigma_z + w_z = \sigma_z + \text{height}/4.3.\end{aligned}\tag{2.17}$$

The published diffusion parameters for these models were found for short sample averaging times of approximately ten minutes. The data used in this study had averaging times of up to four hours and very large eddies would influence the data by increasing the spread of the average plume. These long wavelengths are evident in plume meandering (Munn, 1966). Turner (1969) suggests using a power law to describe peak to mean ratios using σ 's not adjusted according to Eq. (2.17).

$$\sigma_y' = \sigma_y \left[\frac{\text{Averaging time (minutes)}}{10} \right]^C \quad (2.18)$$

An estimate of C can be made using several pairs of samples taken during the same time period. First it is assumed that the crosswind standard deviation increases linearly downwind.

$$\sigma_y' = x \tan[\sigma_\theta] \quad (2.19)$$

where x is downwind distance and σ_θ is the angular standard deviation of the plume. To eliminate interference by vertical diffusion, allow vertical homogeneity of contamination to a height D. If the source strength is Q, a pair of samples can be determined as

$$x_1 = F_1 Q$$

and

$$x_2 = F_2 Q .$$

The relative concentration, F, is estimated by

$$F_1 = \frac{1}{\sqrt{2\pi} \bar{u} D x_1 \tan[\sigma_\theta]} \exp\left[-\frac{y_1^2}{2x_1^2} \tan^2(\sigma_\theta)\right] \quad (2.20)$$

The tangent of σ_θ can be found as a function of the ratios of samples:

$$\tan^2[\sigma_\theta] = \left[\frac{y_2^2}{2x_2^2} - \frac{y_1^2}{2x_1^2} \right] \ln(x_1 x_1 / x_2 x_2). \quad (2.21)$$

The σ_y' found by Eqs. (2.19) and (2.21) is used in Eq. (2.18) to solve for C. The value of C chosen for stable conditions after examining several cases was 0.63. This would multiply the diffusion parameter, σ_y , as referenced by Turner (ibid.), by 4.7 for a two hour averaging time. For unstable conditions, C was chosen to be 0.4, providing a two hour factor of 2.7. These values are somewhat larger than those listed by Turner which ranged from 0.17 to 0.2 for averaging times of less than two hours.

The working equations used in the analysis which incorporate these options are;

$$T = (\text{Averaging time}/10)^C, \quad (2.22)$$

USPHS-TVA:

$$F = \chi/Q = \frac{1}{2\pi(TC_y x^M y + w_y)(C_z x^M z + w_z)} \exp\left[-\frac{1}{2} \left\{ \frac{y^2}{(TC_y x^M y + w_y)^2} + \frac{H^2}{(C_z x^M z + w_z)^2} \right\}\right], \quad (2.23)$$

and Pasquill-Gifford:

$$F = \chi/Q = \frac{1}{\pi \bar{u}(T\sigma_y + w_y)(\sigma_z + w_z)} \exp\left[-\frac{y^2}{2(\sigma_y + w_y)^2} - \frac{H^2}{2(\sigma_z + w_z)^2}\right]. \quad (2.24)$$

The reflection term of the Pasquill-Gifford treatment is not present because only surface values are considered. Washout and chemical transformation are ignored because the samples were all taken within four miles of the source. Normally this process would be approximated by a half life term (Hilst, 1970),

$$\chi(\text{adjusted}) = \chi \exp\left[-\frac{\ln 2.0}{h} \left(\frac{x}{\bar{u}}\right)\right]. \quad (2.25)$$

The travel time of the contaminant is x/\bar{u} , and the half life is h .

CHAPTER III

VARIATIONAL TECHNIQUE TO FIND OPTIMAL SOURCE AND BACKGROUND VALUES

To estimate pollution patterns, the normal order of development has been: given sampling data and a source inventory, find a diffusion model or diffusion coefficients which best fit the data. A diffusion model found in such a manner is extremely localized and keenly sensitive to meteorological parameters. Also, the source inventories are usually of an undependable nature. The technique to be developed in this chapter uses a different approach--sampling data and any reputable diffusion model are used to optimize a background contamination and the magnitudes of a system of strategically placed hypothetical sources or "pseudo-sources". These optimized parameters are then input to the same model to obtain an estimate of the contamination situation over a grid.

Derivation of Analysis Equations

Each air quality control sample, $\tilde{\chi}_{t,n}$, taken at time t and location n , is assumed to be comprised of a background contamination, χ_b , plus a summation over I pseudo-sources of their strength, Q_i , times the relative concentration, $\chi/Q = F(t,i,n)$, for that sampling time,

$$\tilde{\chi}_{t,n} = \chi_b + \sum_{i=1}^I F(t,i,n) Q_i . \quad (3.1)$$

There can be a differing number of samples with respect to time, therefore the total number of samples, N , is a function of time:

$N(t)$. The relative concentration can be found through one of many analytical diffusion models (Chapter II and Appendix B).

Define the functional, J , as the sum of the errors squared of the estimates as described by Eq. (3.1):

$$J = \sum_T \sum_N \left\{ \alpha \left[\chi_b + \sum_I F(t, i, n) Q_i - \tilde{\chi}_{t, n} \right]^2 \right\} . \quad (3.2)$$

This is a weak constraint (Sasaki, 1970a) because Eq. (3.1) is not assumed to be exactly correct. The weight, α , affects all terms equally and is therefore suppressed.

An optimal solution occurs when the variables, χ_b and Q_i 's, are adjusted such that the functional, J or total squared error, is minimized. When this occurs, J 's variation, δJ , is zero,

$$\delta J = \sum_T \sum_N \left\{ \left[\chi_b + \sum_I F(t, i, n) Q_i - \tilde{\chi}_{t, n} \right] \left[\delta \chi_b + \sum_I F(t, k, n) \delta Q_k \right] \right\} = 0 . \quad (3.3)$$

Since the variations of the variables, $\delta \chi_b$ and δQ 's, are independent, Eq. (3.3) can be separated into a system of $I + 1$ simultaneous equations with $I + 1$ unknowns. For the k th out of I source strengths, Q_k :

$$\sum_T \sum_N \left\{ \left[\chi_b + \sum_I F(t, i, n) Q_i - \tilde{\chi}_{t, n} \right] F[t, k, n] \right\} = 0, \quad k = 1, 2, \dots, I . \quad (3.4)$$

For χ_b :

$$\sum_T \sum_N \left\{ \left[\chi_b + \sum_I F(t, i, n) Q_i - \tilde{\chi}_{t, n} \right] \right\} = 0 . \quad (3.5)$$

The system (3.4) and (3.5) comprises the analysis equations for this technique and are termed the Euler-Lagrange equation. Their linearity makes

sequential Gauss-Siedel relaxation (McCracken-Dorn, 1964) applicable for their solution. The recursion formula for the $(m+1)$ th guesses are

for Q_k :

$$Q_k^{(m+1)} = Q_k^{(m)} - \gamma_1 \sum_T \sum_N \{ [\chi_b + \sum_I F(t, i, n) Q_i^{(m)} - \tilde{\chi}_{t, n}] \} / \sum_T \sum_N [F(t, k, n)]^2. \quad (3.6)$$

For χ_b :

$$\chi_b^{(m+1)} = \chi_b^{(m)} - \gamma_2 \sum_T \sum_N \{ [\chi_b^{(m)} + \sum_I F(t, i, n) Q_i - \tilde{\chi}_{t, n}] \} / \sum_t N(t). \quad (3.7)$$

The relaxation factors are γ_1 and γ_2 . There was some experimentation with these where values from 0.1 to 2 were used for each and the most rapid convergence occurred for $\gamma_1 = \gamma_2 = 1$.

Because negative values for background contamination and source strengths are unrealistic, all unknowns must be required to converge to nonnegative values. The first attempt to avoid the negativeness was a substitution of $\chi_b = \chi_b'^2$ and $Q = q^2$ into Eq. (3.2) and then deriving a new set of Euler-Lagrange equations. This approach was unsatisfactory because the iterating was unstable since the analysis equations were nonlinear. The scheme which was later adopted was to reset a parameter to zero if it was corrected to a value of less than zero for any iteration. This method enabled the numerical solution to converge to a satisfactory value.

Analysis of Input Error

A measure of the worth of the Euler-Lagrange Eqs. (3.4) and (3.5) is their ability to filter out the error in the samples. Suppose each sample is comprised of a true value, $\tilde{\chi}_{\text{true}}$, plus a random error, $\epsilon(i, n)$.

$$\tilde{\chi}_{i, n} = \tilde{\chi}_{\text{true}}(i, n) + \epsilon(i, n)$$

Substitution into the analysis equations and separating the terms yields:

$$\left[\sum_T \sum_N \chi_b F(t,k,n) + \sum_T \sum_N \sum_I Q_i F(t,i,n) F(t,k,n) \right. \\ \left. - \sum_T \sum_N [\tilde{\chi}_{\text{true}}(i,n) + \epsilon(i,n)] F(t,k,n) \right] = 0, \quad k = 1, I \quad (3.8)$$

and

$$\sum_T \sum_N \chi_b + \sum_T \sum_N \sum_I Q_i F(t,i,n) - \sum_T \sum_N [\tilde{\chi}_{\text{true}}(i,n) + \epsilon(i,n)] = 0. \quad (3.9)$$

The last terms of (3.8) and (3.9) can be rewritten as

$$- \sum_T \sum_N [\tilde{\chi}_{\text{true}}(i,n) + \epsilon(i,n)] = - \sum_T \sum_N [\tilde{\chi}_{\text{true}}(i,n) - \sum_T \sum_N \epsilon(i,n)] \\ = - \sum_T \sum_N [\tilde{\chi}_{\text{true}}(i,n)] \quad (3.10)$$

and

$$- \sum_T \sum_N [\tilde{\chi}_{\text{true}}(i,n) + \epsilon(i,n) F(t,k,n)] = \sum_T \sum_N [\tilde{\chi}_{\text{true}}(i,n) F(t,k,n) \\ - \sum_T \sum_N \epsilon(i,n) F(t,k,n)] = \sum_T \sum_N [\tilde{\chi}_{\text{true}}(i,n) F(t,k,n)], \quad (3.11)$$

because the expected value of $\epsilon(i,n)$ is zero.

This is justified as long as sample sizes are sufficiently large. Very small samples could add a random bias to the analysis which would show up as an altered background contamination.

CHAPTER IV

A VARIATIONAL LOW-PASS FILTER

The objective analysis found by the technique described in the last chapter will be close to the true field in the downwind distance scale of the data. Near to the area containing the pseudo-sources, however, one can expect erroneous spikes in the analysis because of micro-scale diffusion being estimated through variational optimization of meso-scale data. This chapter describes the filter which is implemented to remove these spikes while at the same time leaving large scale diffusion phenomena unaffected, i.e., a low-pass filter. The method outlined below enables the exact specification of a filtering characteristic while incorporating true data and the optimal guess in the analysis.

The variational filter used is a simple coupling of an observational constraint, an optimal guess constraint as found through the techniques described in Chapter III, a first order and a second order smoothing constraint. The first two constraints tend to hold the analyzed field to the air quality data and the optimal guess, respectively (Sasaki, 1970a). The first order constraint minimizes the slope throughout the analyzed pattern and the second order constraint has the effect of smoothing out the curvature of the analyzed field. This last constraint is similar to the cubic spline term (Fritsch, 1971; Wagner, 1971; Sheets, 1972). A spline is the curve, in this case concentration pattern, passing through discrete points which has the minimum strain energy. This occurs when

$$\int_s \kappa^2 ds = \text{minimum} . \quad (4.1)$$

The arc length is s and κ is the curvature which is a function of the second derivative of concentration with respect to distance.

The variational formalism which includes these constraints in nondimensional continuous form is

$$\begin{aligned} \delta \int_{\Omega} \{ & \tilde{\alpha}_1 (\chi - \tilde{\chi})^2 + \tilde{\alpha}_2 (\chi - \chi')^2 + \beta_1 [(\nabla_x \chi)^2 + (\nabla_y \chi)^2] \\ & + \beta_2 [(\nabla_{xx} \chi)^2 + 2(\nabla_{xy} \chi)^2 + (\nabla_{yy} \chi)^2] \} d\Omega = 0 , \end{aligned} \quad (4.2)$$

where δ describes the continuous variational operation (Sasaki, 1970a).

The horizontal x, y domain is represented by Ω and the tilda and prime distinguish data and optimized guess input. The scaled weights $\tilde{\alpha}_1, \tilde{\alpha}_2, \beta_1$ and β_2 assign priority to each of the respective constraints. If there is no air quality control data at a point, which is usually the case, $\tilde{\alpha}_1 = 0$. To preserve symmetry, the cross derivative has been retained in the spline or second order smoothing constraint.

The analysis equation derived from (4.2) is (see Appendix C for details of derivation):

$$\begin{aligned} & \tilde{\alpha} (\chi - \tilde{\chi}) + \tilde{\alpha}_2 (\chi - \chi') - \beta_1 (\nabla_{xx} \chi + \nabla_{yy} \chi) \\ & + \beta_2 (\nabla_{xxxx} \chi + 2\nabla_{xxyy} \chi + \nabla_{yyyy} \chi) = 0. \end{aligned} \quad (4.3)$$

This can be solved numerically as a boundary value problem. Proof of convergence is shown in Appendix D.

Characteristics of the Filter

The monotonic response of various wavelengths of sinusoidal patterns to Eq. (4.2) is well documented by Wagner (ibid). Although air

pollution patterns are approximated by a Gaussian distribution, Wagner's analysis can be explained. To simplify the investigation of non-sinusoidal response, limit considerations to one dimension:

$$\tilde{\alpha}_1(\chi - \tilde{\chi}) + \tilde{\alpha}_2(\chi - \chi') - \beta_1 \nabla_{xx} \chi + \beta_2 \nabla_{xxxx} \chi = 0. \quad (4.4)$$

Allow a plume to diffuse in the x-direction and describe the nondimensional profile of data and optimal guess by a Gaussian profile.

$$\tilde{\chi} = \chi' = \tilde{C} \exp(-ax^2) \quad (4.5)$$

Expansion of (4.5) into a Fourier series gives (Churchill, 1969)

$$\tilde{\chi} = \chi' = \frac{1}{2} a_0 + \sum_{n=1}^{\infty} (a_n \cos \frac{2n\pi x}{L} + b_n \sin \frac{2n\pi x}{L}), \quad (4.6)$$

where L is the size of the x-domain. If a pattern is symmetric with respect to the origin, $x=0$, Eq. (4.6) is an even function (ibid.) and the sine term should vanish. The analyzed field, χ , is assumed to have the solution

$$\chi = \frac{1}{2} A_0 + \sum_{n=1}^{\infty} A_n \cos \frac{2n\pi x}{L}. \quad (4.7)$$

Substitution of (4.7) and the abbreviated form of (4.6) into (4.4) gives the solution for A_n

$$A_n = a_n / [1 + \frac{\beta_1}{(\tilde{\alpha}_1 + \tilde{\alpha}_2)} (\frac{2n\pi}{L})^2 + \frac{\beta_2}{(\tilde{\alpha}_1 + \tilde{\alpha}_2)} (\frac{2n\pi}{L})^4]. \quad (4.8)$$

If R_n is defined as the monotonic response for the n^{th} harmonic, then

$$R_n = A_n / a_n = \frac{1}{[1 + \frac{\beta_1}{(\tilde{\alpha}_1 + \tilde{\alpha}_2)} (\frac{2n\pi}{L})^2 + \frac{\beta_2}{(\tilde{\alpha}_1 + \tilde{\alpha}_2)} (\frac{2n\pi}{L})^4]}. \quad (4.9)$$

Eq. (4.9) describes the reduction in amplitude of the n^{th} harmonic due to an analysis performed by the one dimensional Euler-Lagrange Eq. (4.4).

The value of R_n ranges from 0 for $n = \infty$, to 1 for $n = 0$. Because $R_0 = 1$, the average value of the filtered field is the same as the nonfiltered.

The effect of a filter on a Gaussian plume can be seen analytically. A widely dispersed plume has a small coefficient (a) of Eq. (4.5) and, conversely, a compact plume has a large (a). In this case the analytical solution to the n^{th} Fourier coefficient, a_n , is

$$\begin{aligned} a_n &= \frac{2}{L} \int_{-L/2}^{L/2} \tilde{C} \cos\left(\frac{2n\pi x}{L}\right) \exp(-ax^2) dx \\ &= \frac{2\tilde{C}B}{L\sqrt{a}} \exp\left(-\frac{n^2\pi^2}{L^2a}\right), \end{aligned} \quad (4.10)$$

where B is a constant of integration which approaches π as L approaches ∞ . This infers that a compact plume (large a) has a greater contribution from the higher harmonics than the dispersed plume. Therefore, to filter out the effects of an undispersed plume, these higher harmonics should be diminished to a greater degree than the lower harmonics. These criteria are fulfilled by Eq. (4.9).

Fig. 1 shows the results of a test which found the total response of the mode concentration as a function of plume width for various weight combinations. For convenience, the abscissa is the nondimensionalized standard deviation of the plume, σ , which is a function of the parameter (a) of Eq. (4.5):

$$a = \frac{1}{2\sigma^2}. \quad (4.11)$$

The weights $\tilde{\alpha}_1 = 1$, $\tilde{\alpha}_2 = 1$, $\beta_1 = 0.05$ and $\beta_2 = 0.05$ were chosen for most applications. Plumes which had a spread corresponding to a σ of less than 0.25 grid interval (= 100 meters on grid used) would have their peak value reduced to half or less. Plumes with $\sigma \geq 1$ grid interval were virtually unaffected. In some cases there was a problem of convergence to a

realistic solution in the vicinity of a steep concentration gradient.

Fig. 17 is an example of this. The crescent shaped area upwind to the source has a contamination less than background as a result of the filter encountering a steep concentration gradient in this region. Cases which demonstrated this problem, however, were rerun with the β_2 weight changed to 0.005. There is slightly less steepness of response for this configuration, but this application generally converged to a realistic solution.

Numerical Solution to Low Pass Analysis Equation

In applying (4.3) numerically as a boundary value problem, the continuous nondimensional operator, ∇ , is replaced by Ψ , a nondimensional centered space finite difference operator, where

$$\Psi_{xx} \chi(i,j) = \chi(i-1,j) + \chi(i+1,j) - 2\chi(i,j) , \quad (4.12)$$

$$\Psi_{yy} \chi(i,j) = \chi(i,j-1) + \chi(i,j+1) - 2\chi(i,j) , \quad (4.13)$$

$$\begin{aligned} \Psi_{xxxx} \chi(i,j) &= \chi(i-2,j) + \chi(i+2,j) - 4[\chi(i-1,j) + \chi(i+1,j)] \\ &\quad + 6\chi(i,j) , \end{aligned} \quad (4.14)$$

$$\Psi_{xxyy} \chi(i,j) = \begin{bmatrix} \chi(i-1,j-1) + \chi(i-1,j+1) + \chi(i+1,j-1) + \chi(i+1,j+1) \\ - 2[\chi(i-1,j) + \chi(i,j-1) + \chi(i+1,j) + \chi(i,j+1)] \\ + 4\chi(i,j) \end{bmatrix} , \quad (4.15)$$

and

$$\begin{aligned} \Psi_{yyyy} \chi(i,j) &= \chi(i,j-2) + \chi(i,j+2) - 4[\chi(i,j-1) + \chi(i,j+1)] \\ &\quad + 6\chi(i,j) . \end{aligned} \quad (4.16)$$

This scheme cannot be applied to the outer two grid points because of the

fourth order finite difference algorithm. Therefore, these points are held to the original analysis. Also, the outermost points must remain unadjusted because this is a boundary value problem and the natural boundary conditions are applied. The mesh size used was 20 by 20 allowing ample space inside this border for a solution.

Each grid point has an optimal guess value, χ' , assigned to it as found by the optimization technique. Air monitoring data were assigned to the nearest grid point. Most of the grid points had no monitoring data; therefore the weight $\tilde{\alpha}_1$ was usually zero.

Liebmann sequential relaxation was applied to solve (4.3). The recursion formula had a relaxation factor equal to one.

$$\chi^{(n+1)} = \chi^{(n)} - \text{Residual} / (\tilde{\alpha}_1 + \tilde{\alpha}_2 + 4\beta_1 + 20\beta_2) \quad (4.17)$$

The analysis was considered a solution when the maximum residual was less than 0.001. This corresponds to an unscaled sensitivity of 0.001 micrograms per cubic meter. The scheme converged in less than 20 passes for the weights used.

CHAPTER V

AIR POLLUTION DATA

A valid test of the analysis techniques should involve sampling data with the following characteristics:

1. The data should be from an area with an isolated source.
2. The area adjacent to the source should have an uncomplicated topography.
3. The source size should approach a point.
4. Although the analysis scheme can handle data as sparse as one measurement per time period, it would be better to have several simultaneous measurements per time period available.
5. The chemical analysis of the data must be as precise as possible with little time delay between collection and analysis.

Blackwell Zinc Company

In the summer of 1971, an ideal situation developed where all of the above criteria were satisfied. The Blackwell Zinc Company (See Fig. 3), which is located in northcentral Oklahoma, arranged to have an air quality surveillance program conducted by the Department of Civil Engineering, the University of Oklahoma. The purpose of the survey was to determine if, and by how much, the ambient air standards were being exceeded.

A computer drawn map of the Blackwell area is shown in Fig. 2.

The surrounding terrain is flat with cultivated fields. The greatest roughness is in the city of Blackwell itself (1970 census: 8,645) to the east of the factory. There are slight depressions in the topography, the most obvious being the Chikaskia River which meanders to the north and east of the city. These could allow residual pockets of contamination during periods of poor ventilation.

It was decided to use the SO_2 data in this study. Most of the SO_2 is emitted from a 308 ft. stack* satisfying the point source criteria. The other data are of an extremely sensitive nature due to legal proceedings. Although all the surveillance data were confidential at the time of this writing, the plant manager gave permission to use the SO_2 data obtained for August, 1971, in this project.

The SO_2 data of August used sampling times ranging from one and one half to four hours. Three samples were taken simultaneously at points roughly downwind, slightly across wind and completely off the average downwind track. The chemical analysis scheme was the West-Gaeke method (U.S. Department of Health, Education, and Welfare, 1965). This method has a 98 percent collection efficiency and detected an upwind concentration, presumably background, as low as one part per ten billion (0.293 micrograms per cubic meter.):**. The method provides an accuracy of $\pm 10\%$ in the range 0.005 to 0.10 ppm (14.8 to 293 micrograms per cubic meters) with increasing accuracy in the range 0.1 to 2 ppm. (ibid.) Many of the samples taken were less than 0.005 ppm which no doubt added a great deal of error to the smaller

*Personal communication with R.A. Mill, School of Environmental Health, University of Oklahoma.

**Personal communication with J.W. Carter, Department of Civil Engineering, University of Oklahoma.

samples. The chemist** stated that the samples in the background range could only have their order of magnitude determined but this was reproducible.

The 11th and 17th of August were chosen as test dates. Both days are week days and represent one unstable and one stable case which are described in Chapter VI. Table I lists these SO₂ data. The concentrations were converted from ppm to micrograms per cubic meter by the factor 0.0029264 and the values are well within the 1971 National Air Quality standards which are shown in Fig. 10.

**Personal communication with J.W. Carter, Department of Civil Engineering, University of Oklahoma.

CHAPTER VI

METEOROLOGICAL CONDITIONS FOR TWO TEST DAYS

In the month of August, 1971, Oklahoma was characteristically covered by summer time highs and ridges with occasional weak fronts passing through the state. Adequate testing of the scheme described in Chapter III should include both stable and unstable conditions. The days which were chosen are the 11th and 17th of that month.

August 11

On the 11th of August (See Figs. 4 and 5) a mass of cool continental polar air pushed southward behind a weak cold front to replace the continental tropical air over Oklahoma. The front became stagnant and diffuse in the afternoon; however, thunderstorms occurred in the vicinity. The soundings for the day (See Fig. 6 for Oklahoma City soundings) show a nocturnal inversion in the morning with decreasing stability in the afternoon. There was enough surface heating during the afternoon to give an adiabatic lapse rate to 850 mb at Topeka, Kansas, and superadiabatic lapse rate to 850 mb at Dodge City, Kansas, on the afternoon of the eleventh. There was at least a five knot wind at the surface throughout the day.

August 17

On the 17th, Oklahoma was under a strong ridge reaching from a broad high centered over the Great Lakes. Figs. 7 and 8 show

the local surface conditions for 0700 and 1900 CDT. The patterns are a conglomerate of small scale highs and lows in a continental tropical air mass. The stability in the morning was high due to subsidence and radiation (see Fig. 9 for Oklahoma City soundings) but daytime heating obliterated this inversion. Dodge City and Topeka, Kansas, had enough surface heating to provide a shallow superadiabatic layer in the afternoon. The winds in the Blackwell area were light or nil from the southeast providing extremely poor ventilation.

Choice of Meteorological Parameters for Diffusion Estimation

The diffusion models used in conjunction with the variational optimization needed wind and stability data as input parameters. The values which were used had to represent a two to four hour average, therefore, several hourly analyses were needed for each datum. The average wind direction found in this manner was tempered with a guess which was obtained by looking at a plot of pollution data. An estimate of downwind direction from survey data was possible because these data were taken at three sites for each sampling period.

The stability types for the diffusion models were estimated from interpolation among the Dodge City, Topeka, and Oklahoma City soundings and a method described by Turner (1969). Turner estimates stability through use of incoming solar radiation, cloud cover, and wind speed in his comprehensive review of Gaussian plume diffusion estimation.

CHAPTER VII

TESTING TECHNIQUES WITH REAL DATA

The Blackwell survey of August, 1971, obtained samples from three locations, the positioning of which was dependent upon the downwind direction. A logical test of the optimization techniques outlined in Chapter III would be to use two locations in the analysis to estimate the third used as a control site. Then, in a harsher test, use one location to estimate the two others. The estimates of the control locations can then be compared with the true values for these sites. Each data configuration was run twice; for the USPHS-TVA and the Pasquill-Gifford models (Eqs. 2-23 and 2-24) to test the sensitivity to differing diffusion estimates.

A 20 x 20 mesh was used with an interval of 400 meters. This enclosed a large interior which would place all the samples within the outer two grid points for smoothing purposes. The maximum residual allowed in the Gauss-Seidel relaxation for the optimization process (Eqs. 3-4 and 3-5) was 1.0×10^{-12} . This represents a sensitivity for the pseudo-sources of 10^{-5} grams per second for $F = \chi/Q$ in the range of 0.01 sec m^{-3} . For the background contamination this gives a sensitivity of 5×10^{-7} micrograms per cubic meter when two samples are used in the analysis. The number of iterations was dependent upon the number of samples used, ranging from eleven for two samples to

150 for twelve. The locations of the samples were given in polar coordinates with the origin at the center of the factory. The factory was placed at the center of the grid and sample grid locations determined through elementary trigonometry.

Preliminary Test Results

Several test runs were completed where the optimal background contamination, χ_b , was forced to zero. These were compared to the same cases with χ_b optimized as originally derived. In all cases error was added as a result of χ_b being forced to zero.

Experiments were performed to determine the best number of pseudo-sources for a given number of input samples. Satisfactory results were still obtained when:

$$\text{Number of pseudo-sources} = \text{Number of samples} - 1, \quad (7.1)$$

and this was shown to be best in practice. Too many pseudo-sources implies too many unknowns for the system (3.4) and (3.5) to solve.

A measure of the poorness of fit of a diffusion model to the true situation is the size of the solved background contamination. A poor modeling attempt, for example, a large error in wind direction, results in a large χ_b . As the modeling attempts deteriorate, χ_b approaches a simple arithmetic average of the input samples and the pseudo-sources approach zero.

One Location Out of Three Used As A Control Site

Three samples from roughly the same time span (hereafter termed 'single period data') were input where each site was used alternately

as a control with the other two input to the optimization analysis. One pseudo-source was assigned to the stack as a point source with an effective height of 150 meters--the other degree of freedom taken by the background contamination. Tables II, III, and IV list several results of using large (approx. $50 \mu\text{gm m}^{-3}$), medium, and small samples (in background range) as controls for the two afternoons and the two diffusion models. The largest errors ($\chi - \hat{\chi}$) occurred when estimating the small control samples. These are less than an order of magnitude smaller than the larger samples. One can argue that a 10% biased error in the chemical analysis of the larger samples used in the variational technique could add 500% error to a control sample in the background range (approx. $1 \mu\text{gm m}^{-3}$).

For most cases the technique had no problem reconstructing larger samples used in the analysis. An exception to this is shown in Table II, the afternoon of the 11th. This is an example of the χ_b being forced to account for almost all of the contamination at the analysis sites. This is attributable to both input samples being on the order of magnitude of background contamination.

Fig. 10 shows a plot of percent error versus sample size for the runs of Tables II, III, and IV. Fig. 11 shows the unfiltered and contoured results valid for the afternoon of the 17th using the optimized parameters listed in Table IV. The USPHS-TVA model was applied in this case. In this and the remaining figures the contours are in proportion to:

$$\text{scaled concentration} = 10 \log_{10}(\chi). \quad (7.2)$$

The maximum concentration is downwind to the factory because of the source's elevation.

The above procedure was repeated using all the data taken during the working hours of the two test days (hereafter termed 'multiple

period data'). Tables V and VI show the results of two runs. In these tables as well as most of the other runs which involved two or more pseudo-sources, the stack location of 150 meters effective height was solved to have all or a large majority of the source strength. This is encouraging because most of the SO_2 contamination originates from the stack. Fig. 12 shows the unfiltered contoured results of Table VI implementing the USPHS-TVA model. In this case the site which had medium sized samples was used as a control. The optimal background contamination was high ($8.42 \mu\text{gm m}^{-3}$). The valid time for Fig. 12 is the same as for Fig. 11 and, except for the backgrounds, the patterns are very similar.

Fig. 13 shows a plot of percent error versus concentration for the runs of Tables V and VI. The larger errors of the multiple period analysis could conceivably be due to fluctuating true source and background strengths throughout the day which are assumed constant in the optimization technique. This problem could be eliminated through intense sampling over short periods.

Two Locations Out of Three Used As Control Data

Data limited to the same time period could not be used in this test because at least 2 input samples are needed in the variational technique. For this reason, only multiple period data were used in this test, inputting one site's data at a time for an analysis which estimated the other sites as controls. Fig. 14 is a plot of error versus concentration for the 17th using the site which reported medium sized concentrations for analysis. The input data were reconstructed closely; however, the accuracy for the control data deteriorated. In this configuration the pseudo-sources were assigned a small or zero value by the optimization technique and the background was roughly equal to a simple arithmetic

mean. The smaller controls show an overestimation and the larger, an underestimation due to an optimal background accounting for much of the contamination. The standard deviation for the analysis data in this case was $1.65 \mu\text{gm m}^{-3}$ whereas the standard deviation for the combined sampling was $19.1 \mu\text{gm m}^{-3}$. A wider variance among the input samples would have helped eliminate this. Fig. 15 shows the unfiltered results which implemented the USPHS-TVA model for the run valid on the morning of the 17th.

The comparison of estimated values of control data with true values shows some error, particularly when only one site was used in the optimization. These errors, however, are in the same order of magnitude as one would expect from the chemical analysis. If the variance of the input data was small, then the optimal χ_b tended to be oversized, increasing the error in the estimates of control data. Therefore, it is recommended that if measurements are taken specifically for application in this technique, they should be well scattered with respect to mean crosswind distance.

CHAPTER VIII

CASE STUDIES

The optimization technique was applied to the survey data of August 11 and 17 using three out of three sample sites in the analysis. Patterns of contamination for a morning and afternoon period were obtained using two data configurations. Single period data from all sampling sites were used in one analysis and the corresponding pattern determined for that period. In the other configuration, multiple period data from the complete working day were used and the resulting optimized Q's and χ_b used to determine the patterns at two valid times. The results listed are from the better of the two diffusion model applications used in each case.

Tables VII and VIII list the results of the optimization technique applied as outlined above. Because a minimum of three samples are used for each, at least two pseudo-sources are solved. Those cases with three samples used two pseudo-source locations at the stack with effective heights 150. and 0.0 meters. The cases which analyzed more than 3 samples optimized a system of pseudo-sources surrounding the stack on the surface as well as several stack locations. All pseudo-sources except the 150 meter high stack location were assigned an initial horizontal and vertical standard deviation, w_y and w_z . These multiple source configurations were usually justified, i.e., the optimal solution had several nonzero

pseudo-source strengths.

The results of August 11, 1971 show more error of the two days. In the vicinity of the frontal zone on this day one would anticipate a variability of wind direction. This would make diffusion estimation difficult and the poor diffusion modeling is shown by the high background contaminations in the first and third tabulations of Table VII. In the second tabulation, which resulted from a single period data input taken after the front had weakened, χ_b is less than the minimum sample as it should be, and the error of the reconstructed samples is small. This indicates a reasonable diffusion estimate was input to the optimization process.

For both days (see Table VIII for the results of the seventeenth) the greatest error is in the analysis done using multiple period data. This arises from the steady state assumption used in the derivation of the optimizing technique. No doubt the source strength varies throughout the day and the author has indeed observed fluctuations in plume strength at the Blackwell plant.

Fig. 16 through 23 show the results of applying the optimized parameters of tables VII and VIII. Because most of the results have more than one nonzero pseudo-source strength, the filter described in Chapter IV was applied to blend the ensemble of plumes at and near the source area.

In comparing the contoured results of the two input data configurations, several discrepancies are found. The fields from the analyses which used single period data input, as well as those which used multiple period data, gave results which were nearly equal in the vicinity of the sample sites. Near the factory, however,

there was some difference--the single period analyses giving a greater concentration gradient in this area. The gradient is exaggerated by the logarithmic scaling. The multiple period analyses (Fig. 20 through 23) show a higher background pollution throughout both days than the single (Figs. 16 through 19) and this accounts for the fewer contours and, at least in part, the looser concentration gradient of the former. The location of maxima are closer to the source area and larger for the single period analyses. It appears that use of multiple period sampling caused a smoothing where mass from peak concentration areas was distributed to areas having only background values. This type of smoothing causes the troublesome error of an erroneously large background which can only be eliminated by a more accurate diffusion estimate.

There are some common characteristics of the two data configuration applications which give credence to the results. In all cases the peak values are located downwind to the factory indicating a sufficient quantity of effluent having originated from an elevated source. This has already been demonstrated in the tabulated solutions of pseudo-source strengths. During very stable conditions one would expect the high values to be located farther downwind and this tendency is demonstrated when comparing morning and afternoon patterns of the same data configurations. The analyses which have the same valid times have similar shapes and, except for high concentrations, similar areas are enclosed. The afternoon of the 17th shows a wider plume for the multiple period analysis than for the corresponding single period analysis, however, both are wider than the norm. Both the single period and multiple period analyses show plumes which are

more spread out across wind for the 17th. This day had very light winds and therefore, the wider averaged plumes are probably a result of the low frequency wind direction fluctuations, or meandering, playing an increased role in dispersion.

CHAPTER IX

CONCLUSIONS AND REMARKS

A variational optimization technique for the mesoscale objective analysis of air pollution was developed and tested. Rather than find a system of diffusion coefficients which best fit a source inventory and receptor sampling, a series of pseudo-sources and background contamination are optimized to best fit a given diffusion model and receptor sampling. This approach has the advantages that no source inventory is necessary and as few as two independent samples can be used, depending upon the number of parameters to be optimized. Further, if one has high confidence in a particular diffusion model, the true value of sources could be estimated.

For the encouraging results shown, there were many poor results which went into their development. A satisfactory analysis was characterized by a smooth convergence of the Gauss-Seidel iterations and a small but nonzero solution to the background contamination. Ideally the background should be less than or equal to the smallest sample involved in the analysis. The confidence in an analysis is further strengthened when the pseudo-sources which correspond to true sources are nonzero. The use of several models or several schemes of determining diffusion coefficients is recommended in an analysis which involves few samples. In this case the true situation cannot be easily

approximated by an ensemble of plumes from a series of pseudo-sources, therefore, the best fitting diffusion model should be chosen. Usually the USPHS-TVA gave the better fit of the two models implemented. The analyses were in general good near the downwind range of the sampling sites, however, near the factory the analyses were in question. The inclusion of a sampling near to the factory would have increased the confidence in the results in this vicinity.

This variational analysis technique appears to be a satisfactory alternative to an expensive dense sampling network. The larger control samples were closely predicted in tests which analyzed samples of large variances. The smaller control samples were predicted within the chemical analysis error bounds. Usually the pseudo-source located above the stack at an effective height of 150 meters was solved to be the major source. This is encouraging because the Blackwell stack does, in fact, account for most of the sulfur dioxide contamination. The pseudo-source strengths determined using the two diffusion models were, in general, similar in size, indicating a degree of insensitivity to the type of model used. The use of a diffusion model in the optimization enables variance to be reproduced. No or little variance in the input data, as in the case when two out of three sites were used as controls, resulted in χ_b approaching a simple arithmetic mean of the analyzed data and the pseudo-source strengths approaching zero.

BIBLIOGRAPHY

- Carpenter, S.B. et al., 1971: Principal plume dispersion models. Journal of The Air Pollution Control Association, Vol. 21, No. 8, pp 491 - 494.
- Changnon, S.A., F.A. Huff and R.G. Semonin, 1971: METROMEX: an investigation of inadvertent weather modification. Bulletin of the American Meteorological Society, Vol. 52, No. 10, pp 958 - 967.
- Churchill, R.V., 1969: Fourier Series and Boundary Value Problems. McGraw-Hill Book Company, New York, N.Y., 248 pp.
- Courant, R. and D. Hilbert, 1926: Methods of Mathematical Physics, Vol. II, John Wiley and Sons, New York, N.Y., 830 pp.
- Egan, B.A. and J.R. Mahoney, 1972: Numerical modeling of advection and diffusion of urban area source pollutants. Journal of Applied Meteorology, Vol. 11, No. 2, pp 312 - 322.
- Fensterstock, J.C. and R.K. Fankhauser, 1968: Thanksgiving 1966 Air Pollution Episode in the Eastern United States. U.S. Department of Health, Education and Welfare; National Air Pollution Control Agency, Raleigh, N.C., 45 pp.
- Fritsch, J.M., 1971: Objective analysis of a two dimensional data field by the cubic spline technique. Monthly Weather Review, Vol. 99, No. 5, pp 379 - 386.
- Gelfand, I.M. and S.V. Fomin, 1963: Calculus of Variations. Translated from Russian by R.S. Silverman, Prentice-Hall, Inc., Englewood Cliffs, N.J., 232 pp.
- Hall, F.P. Jr. and R.R. Hagan, 1971: A Preliminary Case Study of Long Distance Transport of Air Pollution. Paper delivered at the 64th annual meeting of the Air Pollution Control Agency, June 27 - July 1, 1971, Atlantic City, N.J.
- Haltiner, G.J. and F.L. Martin, 1957: Dynamical and Physical Meteorology, McGraw-Hill Book Company, Inc., New York, N.Y., 470 pp.
- Heimbach, J.A., 1971: The correlation of polluted air with tree growth and lung disease in humans. Computers in Biology and Medicine, Vol. 1, pp 243 - 253.

- Hilst, G.F., 1970: Elevation of tracer cloud over an urban area. Proceedings of Symposium on Multiple-Source Urban Diffusion Models, pp. 8-1 to 8-40.
- Lettau, H.H., 1970: Physical and Meteorological Basis for Mathematical Models of Urban Diffusion Processes. Proceedings of Symposium on Multiple-Source Urban Diffusion Models, U.S. Environmental Protection Agency, Air Pollution Control Agency, Research Triangle Park, N.C., pp. 2-1 to 2-26.
- Mahoney, J.R., 1970: Models for the Prediction of Air Pollution. The study group on models for the prediction of air pollution, Organization for Economic Cooperation and Development, Paris, 80 pp.
- Mahoney, J.R., et al., 1970: Analysis of multiple-station urban air sampling data. Proceedings of Symposium on Multiple-Source Urban Diffusion Models, pp. 11-1 to 11-22.
- McCracken, D.D. and W.S. Dorn, 1964: Numerical Methods and Fortran Programming. John Wiley and Sons, Inc., New York, N.Y., 457 pp.
- Montgomery, T.L. and M. Corn, 1967: Adherence of sulfur dioxide concentration in the vicinity of a steam plant to plume dispersion models. Journal of the Air Pollution Control Agency, Vol. 17 No. 8, pp. 512-517.
- Munn, R.E., 1966: Descriptive Micrometeorology. Academic Press, New York, N.Y., 245 pp.
- Pandolfo, J.P., A.A. Marshall and G.E. Anderson, 1971: Prediction by Numerical Models of Transport and Diffusion in an Urban Boundary Layer. The Center for the Environment and Man, Inc., Hartford, Connecticut, 139 pp.
- Roberts, J.J., E.S. Croke, and A.S. Kennedy, 1970: An urban atmospheric dispersion model. Proceedings of Symposium on Multiple-Source Urban Diffusion Models. U.S. Environmental Protection Agency, Air Pollution Control Agency, Research Triangle Park, N.C., pp. 6-1 to 6-72.
- Roberts, O.F.T., 1923: The theoretical scattering of smoke in a turbulent atmosphere. Proceedings of the Royal Society, Series A, Vol. 104, pp. 640-654.
- Ross, L.W., 1970: Simulation of air and water pollution dynamics: a survey. Simulation, Vol. 15, No. 1, pp. 165-169.
- Royal Ministry of Foreign Affairs and Royal Ministry of Agriculture, 1971: Air Pollution Across National Boundaries--The Impact on the Environment of Sulfur in Air and Precipitation. Kungl, Boktryckeriet P.A., Norstedt & Söner 710396, Stockholm, Sweden, 96 pp.

- Sasaki, Y., 1958: An objective analysis based on the variational method. J. Meteor. Soc. Japan, 36, pp. 77-88.
- _____, 1970a: Some basic formalisms in numerical variational analysis. Monthly Weather Review, Vol. 98, No. 12, pp. 875-883.
- _____, 1970b: Numerical variational analysis formulated under the constraints as determined by long wave equations and a low-pass filter. Monthly Weather Review, Vol. 98, No. 12, pp. 884-898.
- _____, 1970c: Numerical variational analysis with weak constraints and application to surface analysis of severe storm gust. Monthly Weather Review, Vol. 98, No. 12, pp. 899-910.
- Sheets, R., 1972: Analysis of Stormfury Data Using the Variational Optimization Approach. Doctoral Dissertation, University of Oklahoma, 145 pp.
- Sutton, O.G., 1953: Micrometeorology, McGraw-Hill Book Company, New York, N.Y., 333 pp.
- Syono, S., 1953: Frequency distribution functions of velocities in turbulent flow. Journal of the Meteorological Society of Japan, Vol. 31, No. a, pp. 1-7.
- Taylor, G.I., 1920: Diffusion by continuous movements. Proceedings of the London Mathematical Society, Vol. 20, pp. 196-212.
- Turner, D.B., 1969: Workbook of Atmospheric Diffusion Estimates. U.S. Department of Health, Education and Welfare, National Air Pollution Control Agency, Cincinnati, Ohio, 84 pp.
- U.S. Atomic Energy Commission, 1968: Meteorology and Atomic Energy 1968. USAEC Division of Technical Information Extension, Oak Ridge, Tenn. 445 pp.
- U.S. Department of Health, Education and Welfare, 1965: Selected Methods for the Measurement of Air Pollutants. PHS Publication No. 999-AP-11, 54 pp.
- Wagner, K.K., 1971: Variational Analysis Using Observational and Low-Pass Filtering Constraints. Master's Thesis, University of Oklahoma, 39 pp.
- Weinstock, R., 1952: Calculus of Variations. McGraw-Hill Book Company, New York, N.Y., 326 pp.
- Wilkins, E.M., 1971: Variational principal applied to numerical objective analysis of urban air pollution distributions. Journal of Applied Meteorology, Vol. 10, No. 5, pp. 974-981.
- Zeidberg, L.D., et al., 1964: The Nashville air pollution study III: morbidity in relation to air pollution. American Journal of Public Health, Vol. 54, No. 1, pp. 85-97.

APPENDIX A

A FUNDAMENTAL SOLUTION FOR FICKIAN DIFFUSION

Fickian diffusion of pollutants in one dimension is written as a linear parabolic equation.

$$\frac{\partial \chi}{\partial t} - K \frac{\partial^2 \chi}{\partial x^2} = 0 \quad (\text{A.1})$$

A fundamental solution to (A.1) is found by first applying the separation of variables technique then integrating the resulting solution over the complete range of eigenvalues.

The separation of variables technique assumes that the solution is a product of two independent functions, $X(x)$ and $T(t)$

$$\chi = X(x)T(t). \quad (\text{A.2})$$

Substitution and separation of the variables gives

$$\frac{T'}{T} = K \frac{X''}{X} = \pm \lambda^2, \quad (\text{A.3})$$

where the constant λ is called an eigenvalue and X is the corresponding eigenfunction. The two resulting equations are an ordinary first order differential equation in t and a second order equation in x . Choosing $-\lambda^2$, their solutions are

$$T = c_1 e^{-\lambda^2 t} \quad (\text{A.4})$$

$$X = c_2 \left(\frac{\sin}{\cos} \right) \lambda x / K^{\frac{1}{2}} \quad (\text{A.5})$$

Use of the cosine term of (A.4) gives the particular solution

$$\chi = c_3 e^{-\lambda^2 t} \cos(\lambda X/K^{1/2}).$$

By integration over the full range of λ , the general solution is written as:

$$\chi = \int_{-\infty}^{\infty} c_3 e^{-\lambda^2 t} \cos(\lambda X/K^{1/2}) d\lambda. \quad (\text{A.6})$$

To integrate (A.6), make the following substitutions:

$$\lambda^2 t = z^2, \quad \lambda = z/t^{1/2}, \quad d\lambda = t^{-1/2} dz, \quad (\text{A.7})$$

$$p = X/(tK)^{1/2}, \quad (\text{A.8})$$

and obtain the integral;

$$\chi = c_3 t^{-1/2} \int_{-\infty}^{\infty} e^{-z^2} \cos(pz) dz \equiv c_3 t^{-1/2} I(p), \quad (\text{A.9})$$

where

$$I'(p) = - \int_{-\infty}^{\infty} e^{-z^2} z \sin(pz) dz. \quad (\text{A.10})$$

Integrating $I'(p)$ by parts gives:

$$I'(p) = - \frac{1}{2p} I(p). \quad (\text{A.11})$$

The integral I has the characteristic of having its derivative a function of the original I . Therefore, I is an exponential function,

$$I(p) = c_4 \exp(-p^2/4), \quad (\text{A.12})$$

and from (A.8) and (A.9), the fundamental solution to Fickian diffusion is determined:

$$\chi = c t^{-1/2} \exp(-x^2/4tK). \quad (\text{A.13})$$

APPENDIX B

GAUSSIAN PLUME MODELING

The average distribution of mass within a cross section of a diffusing puff is assumed to be normally distributed. This Gaussian profile is a valid solution to Fickian diffusion as shown in Chapter II. If it is assumed that diffusion takes place independently in each direction of the Cartesian coordinate system, the puff's concentration profile, χ , is the product of three normal distributions (U.S. Atomic Energy Commission, 1968).

$$\chi(x,y,z) = \frac{Q}{(2\pi)^{3/2} \sigma_x \sigma_y \sigma_z} \exp\left[-\frac{(x - \bar{u}t)^2}{2\sigma_x^2} - \frac{y^2}{2\sigma_y^2} - \frac{z^2}{2\sigma_z^2}\right] \quad (B.1)$$

The instantaneous strength of a source located at 0,0,0 is Q and the σ 's are the standard deviations of the three normal distributions. The quantity $(-\bar{u}t)$ makes (B.1) applicable to the situation where the puff is being blown along x at a speed \bar{u} in a fixed coordinate system.

Equation (B.1) is easily converted to describe diffusion from a continuous source, Q , under steady state conditions. The plume is assumed to be an infinite sum of puffs and downwind diffusion is allowed to be insignificant when compared to transport by the mean wind, \bar{u} . Integrating over $t = \text{zero to infinity}$ gives (ibid.)

$$\chi(x,y,z) = \frac{Q}{2\pi\bar{u}\sigma_y\sigma_z} \exp\left[-\frac{y^2}{2\sigma_y^2} - \frac{z^2}{2\sigma_z^2}\right]. \quad (\text{B.2})$$

Several applications of (B.2) are listed below. The basic difference between them is the manner in which the sigmas are determined. Generally an effective stack height, H , is incorporated into the equations. The problem of the surface interface is solved in a manner similar to heat diffusion theory where an image source is placed beneath the true source (ibid.). This allows perfect reflection at the surface.

$$\begin{aligned} \chi(x,y,z;H) = \frac{Q}{2\pi\bar{u}\sigma_y\sigma_z} \exp\left[-\frac{y^2}{2\sigma_y^2}\right] & \left\{ \exp\left[-\frac{(z-H)^2}{2\sigma_z^2}\right] \right. \\ & \left. + \exp\left[-\frac{(z+H)^2}{2\sigma_z^2}\right] \right\} \end{aligned} \quad (\text{B.3})$$

The Bosanquet-Pearson model, 1936 (Montgomery and Corn, 1967):

$$\chi(x,y,0;H) = \frac{Q}{\sqrt{2\pi}pq\bar{u}x^2} \exp\left[-\frac{y^2}{2q^2x^2} - \frac{H}{px}\right], \quad \sigma_y = qx. \quad (\text{B.4})$$

This version is not strictly binormal. The second exponential is not squared and the denominator does not fit the format of (B.2). The values of p and q range from 0.1 to 0.02 and from 0.16 to 0.04 respectively for moderately turbulent conditions to stable conditions. This equation and the following are written for estimates of surface concentrations only.

The Sutton model, 1947 (Sutton, 1953):

$$\begin{aligned} \chi(x,y,0;H) = \frac{2Q}{\pi C_y C_z \bar{u} x^{(2-n)}} \exp\left[-\frac{1}{x^{(2-n)}} \left(\frac{y^2}{C_y^2} + \frac{H^2}{C_z^2}\right)\right], \quad (\text{B.5}) \\ \sigma_y = \frac{1}{\sqrt{2}} C_y x^{1-n/2}, \quad \sigma_z = \frac{1}{\sqrt{2}} C_z x^{1-n/2}. \end{aligned}$$

C_y and C_z range from 0.21 to 0.08, and n from 0.17 to 0.35 for moderately turbulent to stable conditions.

The modified Sutton model, 1957 (Ross, 1970):

$$\chi(x,y,0;0) = \frac{Q}{2\pi C_y C_z \bar{u} x^{n_y+n_z}} \exp\left[-\frac{1}{2}\left(\frac{y^2}{C_y^2 x^{2n_y}} + \frac{z^2}{C_z^2 x^{2n_z}}\right)\right], \quad (B.6)$$

$$\sigma_y = C_y x^{n_y}, \quad \sigma_z = C_z x^{n_z}.$$

This equation allows effective heights of sources to be located only on the surface ($H=0$).

The Pasquill-Gifford model, 1960 (Turner, 1969):

$$\chi(x,y,0;H) = \frac{Q}{\pi \sigma_y \sigma_z \bar{u}} \exp\left[-\frac{1}{2}\left(\frac{y^2}{\sigma_y^2} + \frac{H^2}{\sigma_z^2}\right)\right]. \quad (B.7)$$

The sigmas are found from graphed values for six stability classes. This model has probably been the most frequently applied model during the 1960's.

The Cramer treatment, 1959 (U.S. Atomic Energy Commission, 1968), uses Equation (B.7), and assumes a power law to find the sigmas:

$$\sigma_y = \sigma_\theta x^p, \quad (B.8)$$

$$\sigma_z = \sigma_\theta x^q.$$

The standard deviation of wind fluctuation is σ_θ . The parameters p and q have values ranging from 0.45 to 0.85 and 0.86 to 1.89, respectively, for values of σ_θ ranging from 3.0 to 25.0 degrees.

The United States Public Health Service - Tennessee Valley Authority model, 1964 (hereafter USPHS-TVA model) (Montgomery and Corn, 1967):

$$\chi(x,y,0;H) = \frac{Q}{2\pi C_y C_z x^{(M_y+M_z)}} \exp\left[-\frac{1}{2}\left(\frac{y^2}{C_y^2 x^{2M_y}} + \frac{H^2}{C_z^2 x^{2M_z}}\right)\right], \quad (B.9)$$

$$\sigma_y = C_y x^{M_y}, \quad \sigma_z = C_z x^{M_z}.$$

For moderate to average turbulence M_y and M_z are both equal to 0.75, C_y is $-0.101167 - 0.15439\bar{u}$ and C_z equals $-0.141965 - 0.011797\bar{u}$. For low turbulence M_y , M_z , C_y and C_z are 0.62, 0.30, 1.5, and 12.0 respectively. The units in this treatment are feet and seconds.

Green's function (Roberts, et al., 1970):

$$\chi(t, t') = \frac{Q}{(2\pi)^{3/2} \sigma_x(t-t') \sigma_y(t-t') \sigma_z(t-t')} \exp\left\{ -\frac{[x - u(t-t')]^2}{2\sigma_x^2} - \frac{y^2}{2\sigma_y^2} - \frac{z^2}{2\sigma_z^2} \right\}. \quad (B.10)$$

This equation closely resembles (B.1). It describes the dispersion of a single puff emitted instantaneously at time t' after travelling a distance $\bar{u}(t-t')$. The vertical and horizontal sigmas, σ_y , σ_z , in the cited reference are the same as for the Pasquill-Gifford model and σ_x is set equal to σ_y . Eq. (B.10) may be used to estimate diffusion from a continuous source by summing a finite number of puffs. The advantage of such an application is that a varying mean wind can be incorporated and therefore, large transport distances may be employed.

APPENDIX C

DERIVATION OF EULER-LAGRANGE EQUATION FOR LOW-PASS FILTER

In the application of variational calculus presented in Chapter IV, the error represented by the functional J is minimized. J is a function of the data, guess field, first order and second order constraints (Eq. 4.2):

$$J = \int_{\Omega} \{ \tilde{\alpha}_1 (\chi - \tilde{\chi})^2 + \tilde{\alpha}_2 (\chi - \chi')^2 + \beta_1 [(\nabla_x \chi)^2 + (\nabla_y \chi)^2] + \beta_2 [(\nabla_{xx} \chi)^2 + 2(\nabla_{xy} \chi)^2 + (\nabla_{yy} \chi)^2] \} d\Omega. \quad (C.1)$$

The analyzed contamination, χ , is optimized when J is minimal. This occurs when J 's variation, δJ , is equal to zero. Carrying through the operation:

$$\delta J = 2 \int_{\Omega} \{ \tilde{\alpha}_1 (\chi - \tilde{\chi}) \delta \chi + \tilde{\alpha}_2 (\chi - \chi') \delta \chi + \beta_1 [\nabla_x \chi \delta \chi + \nabla_y \chi \delta \chi] + \beta_2 [\nabla_{xx} \chi \nabla_{xx} \delta \chi + 2 \nabla_{xy} \chi \nabla_{xy} \delta \chi + \nabla_{yy} \chi \nabla_{yy} \delta \chi] \} d\Omega. \quad (C.2)$$

If natural boundary conditions hold, the following commutative law applies.

$$\nabla_i \chi \nabla_j \delta \chi = - \nabla_i \nabla_j \chi \delta \chi \quad (C.3)$$

This is easily shown by parts integration of (C.2). The so-called natural boundary conditions force the parts integration term which is integrated over the boundary to zero. Usually this is accomplished by allowing no variation along the boundary ($\delta \chi = 0$). With air pollution applications this can be validated by solving over a large enough space so that the boundaries are assumed to have either a zero or a steady background concentration.

Eq. (C.2) can then be written as

$$\begin{aligned} 2 \int_{\Omega} \{ \tilde{\alpha}_1 (\chi - \tilde{\chi}) + \tilde{\alpha}_2 (\chi - \chi') - \beta_1 (\nabla_{xx} \chi + \nabla_{yy} \chi) \\ + \beta_2 (\nabla_{xxxx} \chi + 2 \nabla_{xxyy} \chi + \nabla_{yyyy} \chi) \} \delta \chi d\Omega = 0, \end{aligned} \quad (C.4)$$

A nontrivial solution has the $\{ \}$ portion of (C.4) equal to zero, therefore

$$\begin{aligned} \tilde{\alpha}_1 (\chi - \tilde{\chi}) + \tilde{\alpha}_2 (\chi - \chi') - \beta_1 (\nabla_{xx} \chi + \nabla_{yy} \chi) \\ + \beta_2 (\nabla_{xxxx} \chi + 2 \nabla_{xxyy} \chi + \nabla_{yyyy} \chi) = 0, \end{aligned} \quad (C.5)$$

which is termed the Euler-Lagrange or analysis equation.

APPENDIX D

CONVERGENCE OF LOW-PASS FILTER

The proof of convergence for the filtering technique is analogous to the method described by Sasaki (1970c). If the true solution to the Euler-Lagrange Eq. (4.3) is χ_t , then the error after iteration m is $\Delta\chi^{(m)} = \chi^{(m)} - \chi_t$. Eq. (4.3) is a linear operator acting on χ , therefore

$$L(\chi^{(m)}) = L(\chi^{(m)}) - L(\chi_t) = L(\chi^{(m)} - \chi_t) = L(\Delta\chi^{(m)}) = R^{(m)}, \quad (D.1)$$

where $R^{(m)}$ is the residual equation at pass m :

$$\begin{aligned} R^{(m)} = & (\tilde{\alpha}_1 + \tilde{\alpha}_a) \Delta\chi^{(m)} - \beta_1 (\nabla_{xx} \Delta\chi^{(m)} + \nabla_{yy} \Delta\chi^{(m)}) + \beta_2 (\nabla_{xxxx} \chi^{(m)} \\ & + 2\nabla_{xx} \nabla_{yy} \chi^{(m)} - \nabla_{yyyy} \chi^{(m)}). \end{aligned} \quad (D.2)$$

If the error at iteration number $m+1$ is determined using Richardson or simultaneous relaxation,

$$\Delta\chi^{(m+1)} = \Delta\chi^{(m)} - \frac{R^{(m)}}{(\tilde{\alpha}_1 + \tilde{\alpha}_a - \frac{4\beta_1}{\Delta s^2} + \frac{20\beta_2}{\Delta s^4})}, \quad (D.3)$$

where a symmetrical grid is assumed:

$$\Delta x = \Delta y = \Delta s.$$

If the solution is convergent, then the error of the $(m+1)$ th guess must be less than or equal to that of the m th guess. Therefore,

the amplification factor, G , as defined in Eq. (D.4) must be ≤ 1 :

$$\Delta X^{(m+1)} = G \Delta X^{(m)}. \quad (D.4)$$

The error pattern for the m^{th} guess can be expressed by a simple two dimensional harmonic:

$$\Delta X^{(m)} = e^{i\mu x + i\eta y}.$$

Upon substitution, the centered space finite difference operators (4.12) through (4.16) can be written as

$$\psi_{xx} = [-4\sin^2(\mu\Delta x/2)]\Delta s^2, \quad (D.5)$$

$$\psi_{yy} = [-4\sin^2(\eta\Delta y/2)]\Delta s^2, \quad (D.6)$$

$$\psi_{xxxx} = [16\sin^4(\mu\Delta x/2)]\Delta s^4, \quad (D.7)$$

$$\psi_{yyyy} = [16\sin^4(\eta\Delta y/2)]\Delta s^4, \quad (D.8)$$

$$2\psi_{xxyy} = [32\sin^2(\mu\Delta x/2)\sin^2(\eta\Delta y/2)]\Delta s^4. \quad (D.9)$$

The residual equation for the m^{th} guess is then

$$\begin{aligned} R^{(m)} = & \Delta X^{(m)} \{ (\tilde{\alpha}_1 + \tilde{\alpha}_2) - 4\beta_1 [-\sin^2(\mu\Delta x/2) - \sin^2(\eta\Delta y/2)]/\Delta s^2 \\ & + \beta_2 [16(\sin^4(\mu\Delta x/2) + \sin^4(\eta\Delta y/2)) \\ & + 32\sin^2(\mu\Delta x/2)\sin^2(\eta\Delta y/2)]/\Delta s^4 \}. \end{aligned} \quad (D.10)$$

The $(m+1)^{\text{th}}$ guess for the error is in the form

$$\Delta X^{(m+1)} = \Delta X^{(m)} - \frac{\Delta X^{(m)} B}{D} = \Delta X^{(m)} \left[\frac{D-B}{D} \right], \quad (D.11)$$

and a value for G is obtained by combining Eqs. (D.4), (D.10) and (D.11):

$$G = \frac{\left[\beta_1 [-4(\sin^2(\mu\Delta x/2) + \sin^2(\eta\Delta y/2)) + 4]/\Delta s^2 - \beta_2 [16(\sin^4(\mu\Delta x/2) + \sin^4(\eta\Delta y/2)) + 32\sin^2(\mu\Delta x/2)\sin^2(\eta\Delta y/2) - 20]/\Delta s^4 \right]}{[\tilde{\alpha}_1 + \tilde{\alpha}_2 + 4\beta_1/\Delta s^2 + 20\beta_2/\Delta s^4]} \quad (D.12)$$

One manner of insuring convergence is to have the respective coefficients for each weight in the numerator be less than or equal to those of the denominator of Eq. (D.12). This criterion occurs unquestionably for all but the β_2 term. With this weight the following must hold for universal convergence:

$$16\sin^4(\mu\Delta x/2) + 16\sin^4(\eta\Delta y/2) + 32\sin^2(\mu\Delta x/2)\sin^2(\eta\Delta x/2) - 20 \leq 20. \quad (D.13)$$

When either μ or $\eta = 0$, i.e., the error function applies in one dimension only, Eq. (D.13) reduces to $16\sin^4(\mu\Delta s/2) \leq 20$ which is true for any μ or η and Δs . When both μ and η are nonzero, (D.13)'s criterion is met if

$$\tilde{\alpha}_1 + \tilde{\alpha}_2 \geq \frac{24\beta_2}{\Delta s^4}, \quad (D.14)$$

as was the case in this study where the quantity $(\tilde{\alpha}_1 + \tilde{\alpha}_2)$ was two orders of magnitude greater than β_2 .

If weights are needed which do not satisfy (D.14), a proper choice of a relaxation factor*, γ_1 , will damp out error propagation where the error recursion formula is

$$\Delta\chi^{(m+1)} = \Delta\chi - \gamma_1 R^{(m)} / [\tilde{\alpha}_1 + \tilde{\alpha}_2 + 4\beta_1/\Delta s^2 + 20\beta_2/\Delta s^4]. \quad (D.15)$$

The β_2 terms are isolated by setting $\tilde{\alpha}_1 = \tilde{\alpha}_2 = \beta_1 = 0$ and γ_1 is solved from (D.15). Convergence is guaranteed for $\gamma_1 \leq 5/8$.

*Personal communication with Y. Sasaki.

TABLE I

BLACKWELL AIR QUALITY CONTROL DATA FROM 11 AND 17 AUGUST, 1971

<u>Date</u>	<u>Location</u>	<u>Time</u>		<u>Concentration</u>	
		<u>Start</u>	<u>Stop</u>	<u>PPM</u>	<u>$\mu\text{gm m}^{-3}$</u>
11	1.7 mi. 270°	0630	1030 (CDT)	0.0017	4.976
		1030	1430	0.0004	1.171
		1430	1830	0.0009	2.634
		1830	2230	0.0007	2.049
	1.5 mi. 0°	0800	1000	0.0010	2.927
		1000	1200	0.0013	3.805
		1400	1600	0.0004	1.171
	1.5 mi. 30°	0815	1015	0.0220	64.392
		1015	1215	0.0194	56.782
		1415	1615	0.0137	40.099
17	1.7 mi. 270°	0615	0815	0.0032	9.366
		0815	1015	0.0038	11.122
		1015	1215	0.0023	6.732
		1215	1415	0.0026	7.609
		1415	1615	0.0035	10.244
		1615	1815	0.0018	5.268
		1815	2015	0.0019	5.561
	1.5 mi. 0°	0600	1000	0.0006	1.756
		1000	1400	0.0004	1.171
		1400	1800	0.0004	1.171
	1.7 mi. 315°	0630	0800	0.0166	48.587
		0830	1000	0.0140	40.977
		1030	1200	0.0201	58.831
		1230	1400	0.0209	61.172
		1430	1600	0.0179	52.391
		1630	1800	0.0164	48.001

The locations of samples are given in polar coordinates, where the origin is at the center of the Blackwell plant and 0° is north. The concentrations represent an average over the respective sampling period.

TABLE II

TESTING OPTIMIZATION USING A LARGE SAMPLE AS CONTROL IN

SINGLE PERIOD ANALYSIS

<u>Period of Sampling</u>	<u>\bar{x} $\mu\text{gm m}^{-3}$</u>	<u>Optimal x $\mu\text{gm m}^{-3}$</u>	<u>% Error</u>	<u>Q gm sec⁻¹</u>	<u>X Background $\mu\text{gm m}^{-3}$</u>
Afternoon of 11th, USPHS-TVA Model:					
1030 - 1430 CDT	1.17	1.17	0.0	5×10^{-5}	1.17
1400 - 1600	1.17	1.17	0.0		
1415 - 1615	40.1*	1.17	-97.1		
Afternoon of 11th, Pasquill-Gifford Model:					
1030 - 1430	1.17	1.17	0.0	2×16^{-5}	1.17
1400 - 1600	1.17	1.17	0.0		
1415 - 1615	40.1*	1.17	-97.1		
Afternoon of 17th, USPHS-TVA Model:					
1615 - 1815	5.27	5.27	0.0	261	0.97
1400 - 1800	1.17	1.17	0.0		
1630 - 1800	48.0*	67.0	-39.6		
Afternoon of 17th, Pasquill-Gifford Model:					
1615 - 1815	5.27	5.27	0.0	381	0.73
1400 - 1800	1.17	1.17	0.0		
1630 - 1800	48.0*	15.3	-68.		

The point pseudo-source with 150 meters effective height was located at the stack site.

*indicates control sample.

TABLE III

TESTING OPTIMIZATION USING A SMALL SAMPLE AS CONTROL IN

SINGLE PERIOD ANALYSIS

<u>Period of Sampling</u>	<u>\bar{x} $\mu\text{gm m}^{-3}$</u>	<u>Optimal \bar{x} $\mu\text{gm m}^{-3}$</u>	<u>% Error</u>	<u>Q gm sec⁻¹</u>	<u>\bar{x} Background $\mu\text{gm m}^{-3}$</u>
Afternoon of 11th, USPHS-TVA Model:					
1030 - 1430 CDT	1.17*	0.94	-19.6		
1400 - 1600	1.17	1.17	0.0	260.	0.93
1415 - 1615	40.1	40.1	0.0		
Afternoon of 11th, Pasquill-Gifford Model:					
1030 - 1430	1.17*	0.0	-100.		
1400 - 1600	1.17	7.78	565.	207.	0.0
1415 - 1615	40.1	38.8	3.31		
Early Afternoon of 17th, USPHS-TVA Model:					
1215 - 1415	7.61	7.61	0.0		
1000 - 1400	1.17*	4.75	306.	226.	3.87
1230 - 1400	61.2	61.2	0.0		
Early Afternoon of 17th, Pasquill-Gifford Model:					
1215 - 1415	7.61	18.1	138.		
1000 - 1400	1.17*	8×10^{-4}	-99.9	152.	0.0
1230 - 1400	61.2	57.9	-5.35		

The point pseudo-source with 150 meters effective height was located at the stack site.

*indicates control sample.

TABLE IV

TESTING OPTIMIZATION USING A MEDIUM SAMPLE AS CONTROL IN
SINGLE PERIOD ANALYSIS

<u>Period of Sampling</u>	<u>\bar{x} $\mu\text{gm m}^{-3}$</u>	<u>Optimal \bar{x} $\mu\text{gm m}^{-3}$</u>	<u>% Error</u>	<u>Q gm sec⁻¹</u>	<u>x Background $\mu\text{gm m}^{-3}$</u>
Afternoon of 11th, USPHS-TVA Model:					
1430 - 1830 CDT	2.63*	0.94	-64.		
1400 - 1600	1.17	1.17	0.0	260	0.94
1415 - 1615	40.1	40.1	0.0		
Afternoon of 11th, Pasquill-Gifford Model:					
1430 - 1830	2.63*	0.0	-100.		
1400 - 1600	1.17	7.78	565.	207.	0.0
1415 - 1615	40.1	38.8	3.30		
Afternoon of 17th, USPHS-TVA Model:					
1615 - 1815	5.27*	4.08	-22.5		
1400 - 1800	1.17	1.17	0.0	185.	1.02
1630 - 1800	48.0	48.0	0.0		
Afternoon of 17th, Pasquill-Gifford Model:					
1615 - 1815	5.27	14.9	184.		
1400 - 1800	1.17	1.45	24.2	126	0.0
1630 - 1800	48.0	47.9	0.02		

The point pseudo-source with 150 meters effective height was located at the stack site.

*indicates control sample.

TABLE V

RESULTS OF MULTIPLE PERIOD ANALYSIS USING ONE CONTROL SITE FOR

11 AUGUST, 1971

<u>Pseudo-Source Location</u>		Effective Height (meters)	Initial Plume Spread		$Q(\text{gm sec}^{-1})$	
Distance from stack (meters)	Direction (Degrees from North)		Assumed (meters)		USPHS-TVA	Pasquill- Gifford
			w_y	w_z		
Stack location		150	0	0	120.	90.0
Stack location		0	10	10	0.0	0.0
200	270	0	20	5	0.0	0.0
200	90	0	20	5	0.0	0.0
Stack location		50	0	5	0.0	0.0

Background = $9.80 \mu\text{gm/m}^3$ for USPHS-TVA.

Background = $8.97 \mu\text{gm/m}^3$ Pasquill-Gifford.

The parameters were solved using the USPHS-TVA and Pasquill-Gifford models. These values resulted from using the samples collected during the working portion of the 11th (0800 - 1800). The control location had samples of small to medium size.

TABLE VI

RESULTS OF MULTIPLE PERIOD ANALYSIS USING ONE CONTROL SITE FOR

17 AUGUST, 1971

Pseudo-Source Location		Effective Height (meters)	Initial Plume Spread		Q(gm sec ⁻¹)	
Distance from stack (meters)	Direction (Degrees from North)		Assumed (meters)		USPHS-TVA	Pasquill- Gifford
			w _y	w _z		
Stack location		150	0	0	204.	94.9
Stack location		0	10	10	0.0	0.0
286	225	0	10	10	0.0	0.0
Stack location		100	0	0	0.0	0.0
286	315	0	10	10	0.0	17.8
200	0	0	10	10	0.0	5.59

Background = $8.42 \mu\text{gm}/\text{m}^3$ for USPHS-TVA.

Background = $7.30 \mu\text{gm}/\text{m}^3$ for Pasquill-Gifford.

The control location had samples of medium size. The rest is the same as Table V.

TABLE VII

SINGLE PERIOD AND MULTIPLE PERIOD ANALYSES FOR 11 AUGUST, 1971

Period of Sampling (CDT)	$\tilde{\chi}$ ($\mu\text{gm m}^{-3}$)	Optimal χ ($\mu\text{gm m}^{-3}$)	% Error	Pseudo-Source Location Direction (Degrees)	Pseudo-Source Distance (Meters)	Pseudo-Source Effective Height (meters)	w_y (m)	w_z (m)	Optimal Pseudo- Source Size (gm sec ⁻¹)
<u>Morning of 11th</u>									
0630 - 1030	4.98	3.84	-22.8	Stack Location		150.	0.0	0.0	0.01
0800 - 1000	2.93	4.07	38.9	Stack Location		0.0	10.0	10.0	70.
0815 - 1015	64.4	64.3	- 0.01	$\chi_b = 3.84 \mu\text{gm m}^{-3}$					
<u>Afternoon of 11th</u>									
1030 - 1430	1.17	1.03	-11.5	Stack Location		150.	0.0	0.0	140.
1400 - 1600	1.17	1.31	11.6	Stack Location		0.0	10.0	10.0	100.
1415 - 1615	40.1	40.1	0.0	$\chi_b = 1.03 \mu\text{gm m}^{-3}$					
<u>Working portion of 11th</u>									
1030 - 1430	1.17	6.98	496.	Stack Location		150.	0.0	0.0	127.
1430 - 1830	2.63	6.98	166.	Stack Location		0.0	10.	10.	0.0
0800 - 1000	2.93	7.15	144.	270	200	0.0	20.	5.0	0.0
1000 - 1200	3.81	13.0	241.	90	200	0.0	20.	5.0	0.0
1400 - 1600	1.17	7.09	506.	Stack Location		50.	0.0	5.0	0.0
0815 - 1015	64.4	76.5	18.7	0	200	0.0	20.	5.0	0.0
1015 - 1215	56.8	31.7	-44.2	180	200	0.0	20.	5.0	0.0
1415 - 1615	40.1	23.6	-41.1	$\chi_b = 6.98 \mu\text{gm m}^{-3}$					

Three sites out of three were used in these analyses of 11 August. The first two tabulations used data from roughly the same time and the last used all the samples from the working hours of the day. On this day there was a great deal of wind variability due to a frontal passage and therefore modeling the diffusion was difficult. This shows up as a large background contamination, χ_b , in the first and last tabulation.

TABLE VIII

SINGLE PERIOD AND MULTIPLE PERIOD ANALYSES FOR 17 AUGUST, 1971

Period of Sampling (CDT)	$\tilde{\chi}$ ($\mu\text{gm m}^{-3}$)	Optimal χ ($\mu\text{gm m}^{-3}$)	%Error	<u>Pseudo-Source Location</u>		Pseudo-Source Effective Height (Meters)	w_y (m)	w_z (m)	Optimal Pseudo- Source Size (gm sec ⁻¹)	
				Direction (Degrees)	Distance (Meters)					
<u>Morning of 17th.</u>										
0815 - 1015	11.1	11.1	0.14	Stack Location		150.	0.0	0.0	2.81	
0600 - 1000	1.76	1.75	-0.69	Stack Location		0.0	30.	5.0	35.6	
0830 - 1000	41.0	41.0	0.01	$\chi_b = 1.75 \mu\text{gm m}^{-3}$						
<u>Afternoon of 17th</u>										
1615 - 1815	5.27	5.03	-4.59	Stack Location		150.	0.0	0.0	33.8	59
1400 - 1800	1.17	1.39	19.0	Stack Location		0.0	30.0	5.0	101.	
1630 - 1800	48.0	48.0	0.04	$\chi_b = 0.816 \mu\text{gm m}^{-3}$						
<u>Working portion of 17th</u>										
0815 - 1015	11.1	8.97	-19.1	Stack Location		150.	0.0	0.0	217.	
1015 - 1215	6.73	6.27	- 6.80	Stack Location		0.0	10.0	10.0	0.0	
1215 - 1415	7.61	8.51	11.8	225	283	0.0	10.0	10.0	0.0	
1415 - 1615	10.2	20.9	105.	Stack Location		100.	0.0	0.0	0.0	
1615 - 1815	5.27	8.51	61.5	315	283	0.0	10.0	10.0	0.0	
1000 - 1400	1.17	5.77	393.	0	200	0.0	10.0	10.0	0.0	
1400 - 1800	1.17	5.10	336.	180	200	0.0	10.0	10.0	0.0	
0830 - 1000	41.0	31.6	-22.8	135	283	0.0	10.0	10.0	0.0	
1030 - 1200	58.8	59.8	1.77	45	283	0.0	10.0	10.0	0.0	
1230 - 1400	61.2	59.8	-2.22	90	200	0.0	10.0	10.0	0.0	
1430 - 1600	52.4	29.4	-43.7	Stack Location		0.0	50.0	5.0	0.0	
1630 - 1800	48.0	59.8	24.7	$\chi_b = 4.93 \mu\text{gm m}^{-3}$						

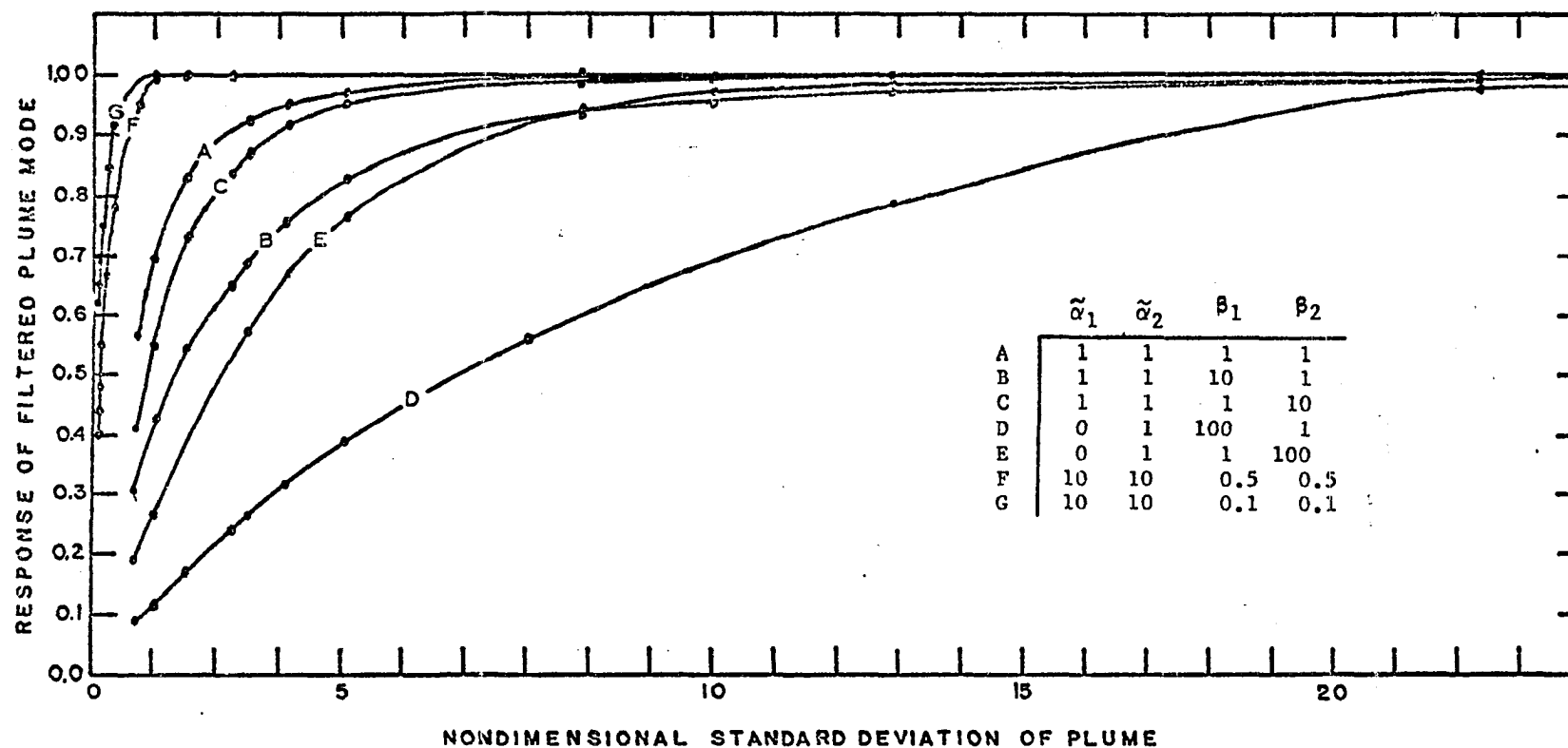


Fig. 1. The response of the mode in the filtered analysis for several weight configurations. The abscissa is the nondimensional standard deviation of the Gaussian distribution and the ordinate is the response. Weight combinations which gave curve F, or very similar to it, were applied for the filtered runs.

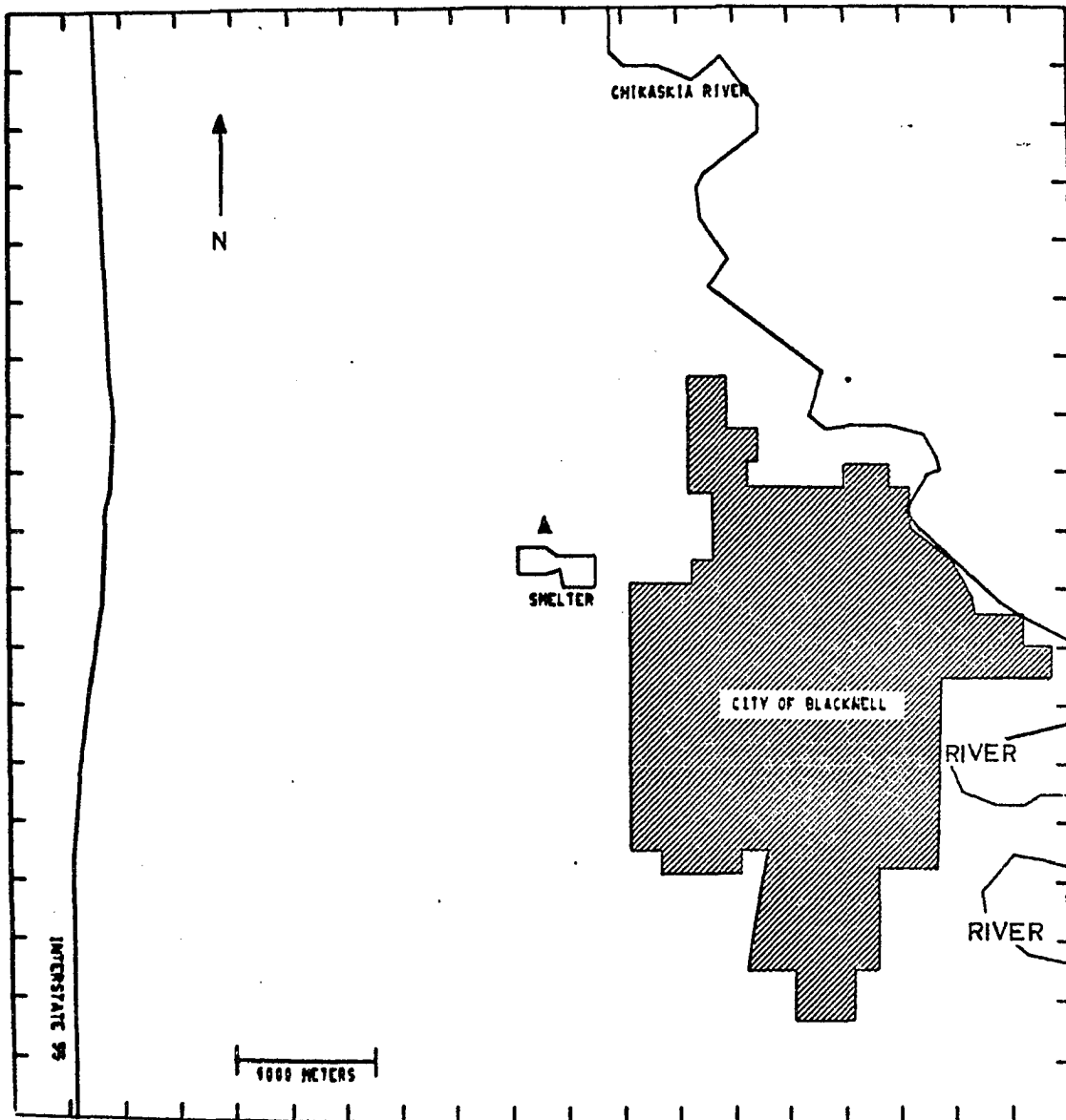


Fig. 2. A map of the Blackwell, Oklahoma, area. The exact center of the map and of the 20 by 20 mesh which is of the same scale, is at the smoke stack of the Blackwell Zinc Company. Interstate route 35, to the left, could provide a small source of SO_2 ; however, the great majority of the SO_2 contamination is from the stack. Distances on the figure were found using a lambert conformal projection with the reference latitude and longitude at the center of the map. The triangle indicates the point from which Fig. 3 was photographed.

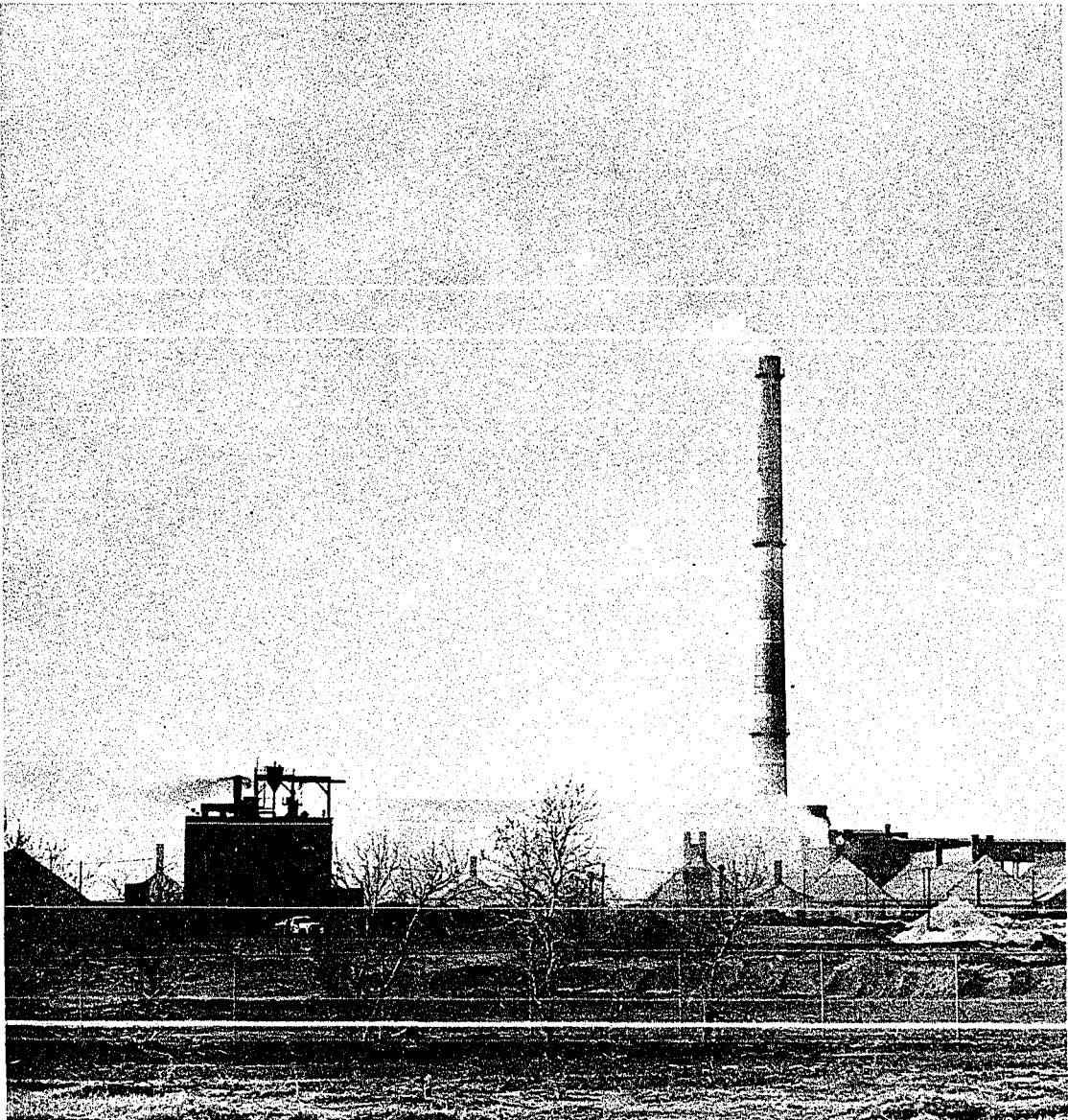


Fig. 3. The Blackwell Zinc Company. The photograph was taken 0840 CST 30 March, 1971. The particulate pollution, which is Blackwell's major problem, can be seen coming from the buildings which house the horizontal retorts. Most of the sulfur dioxide contamination originates from the stack.

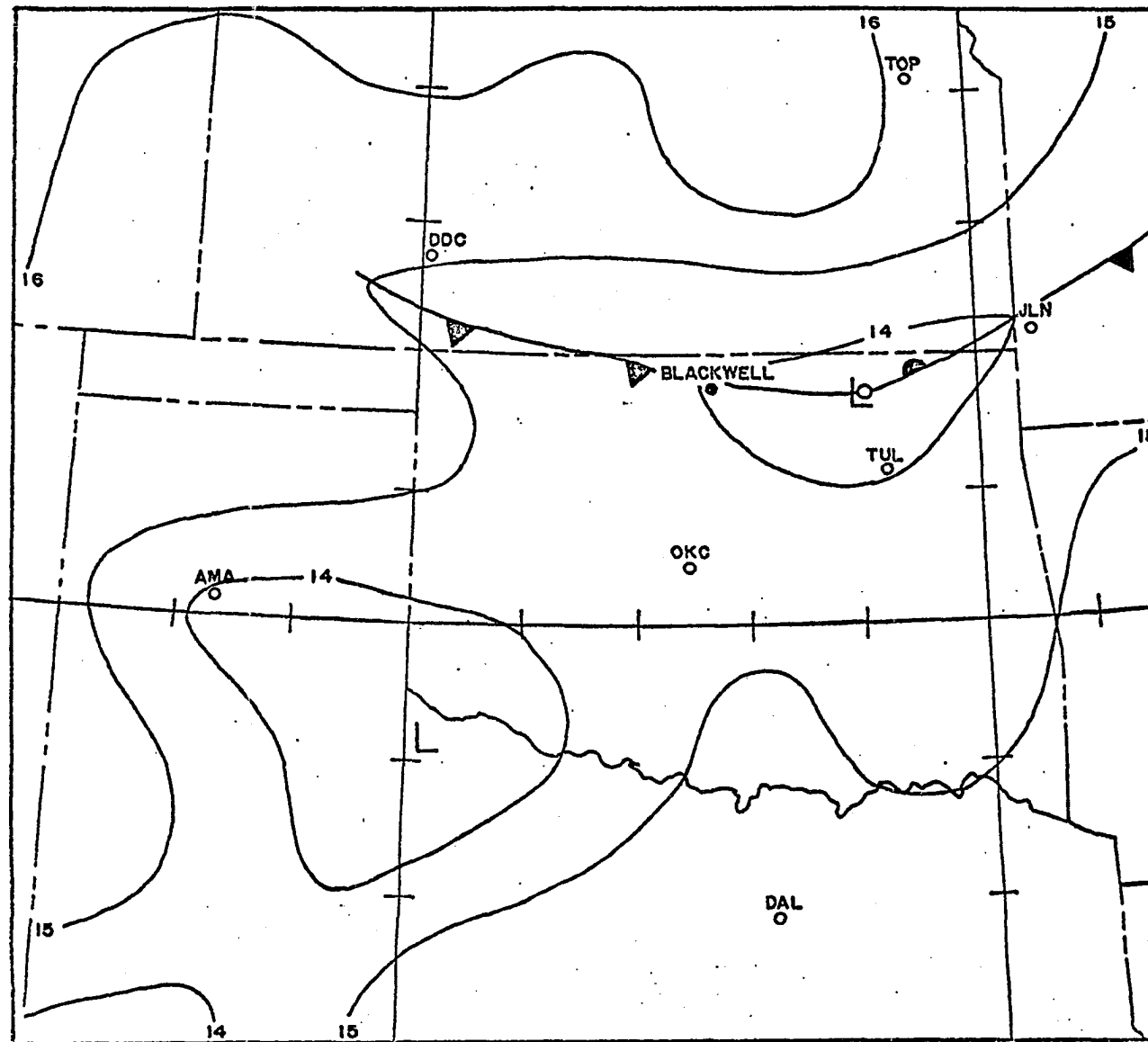


Fig. 4. Surface situation of 11/0700 CDT. A weak cold front was just north of Blackwell and weak thunderstorms were reported along the front from Texas to New York. In Oklahoma and Kansas, however, only cumulonimbus were reported in the early morning.

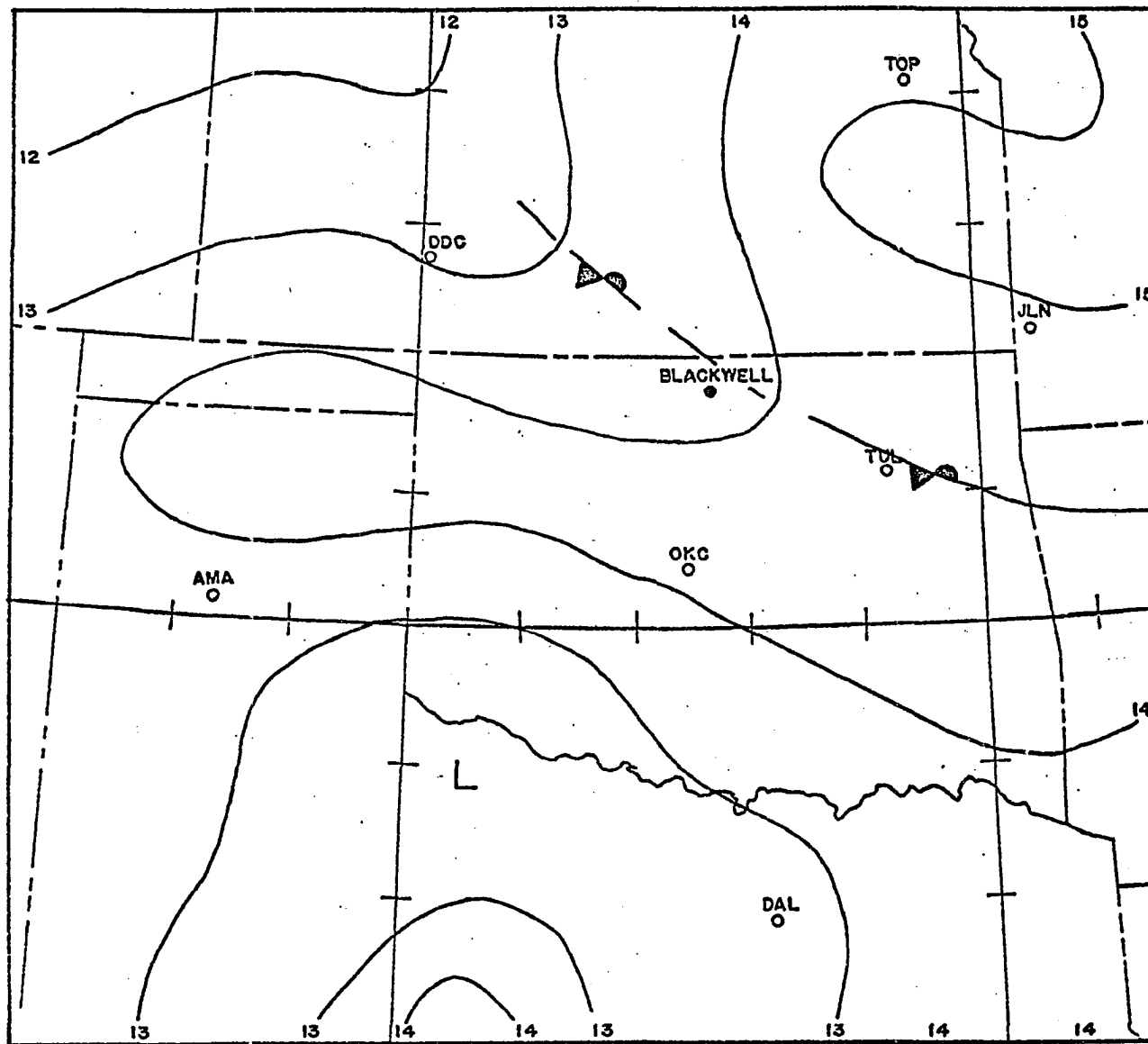


Fig. 5. Surface situation of 11/1900 CDT. The front has become stationary and has weakened in the Blackwell area. Enough heating has occurred in the afternoon to initiate scattered air mass thunderstorms to the south of the front.

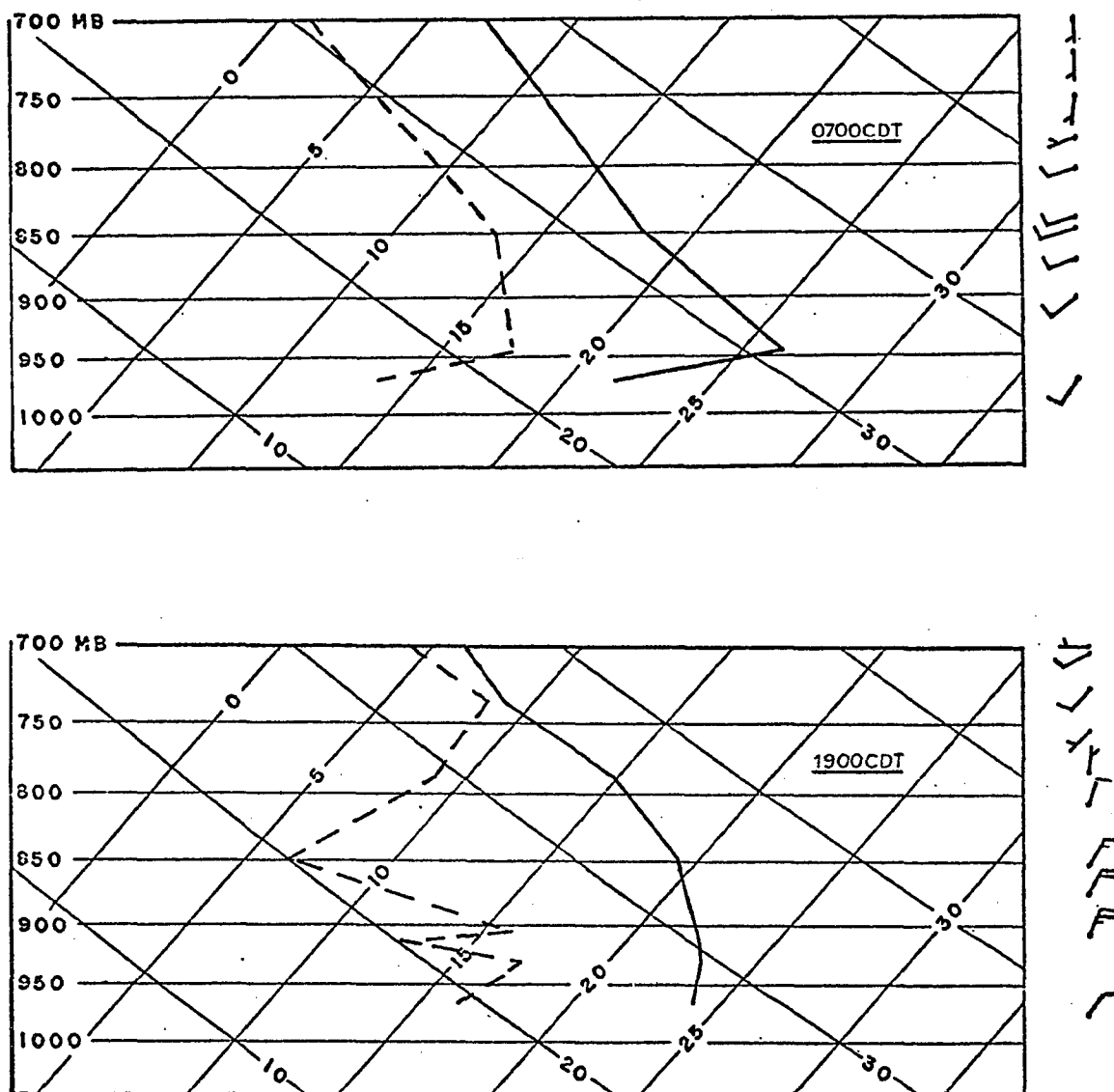


Fig. 6. The morning and afternoon soundings for Oklahoma City (TIK), 11 August, 1971. There is a nocturnal inversion in the morning (11/0700 CDT) with decreasing stability in the afternoon. Convective activity is evident in the afternoon sounding.

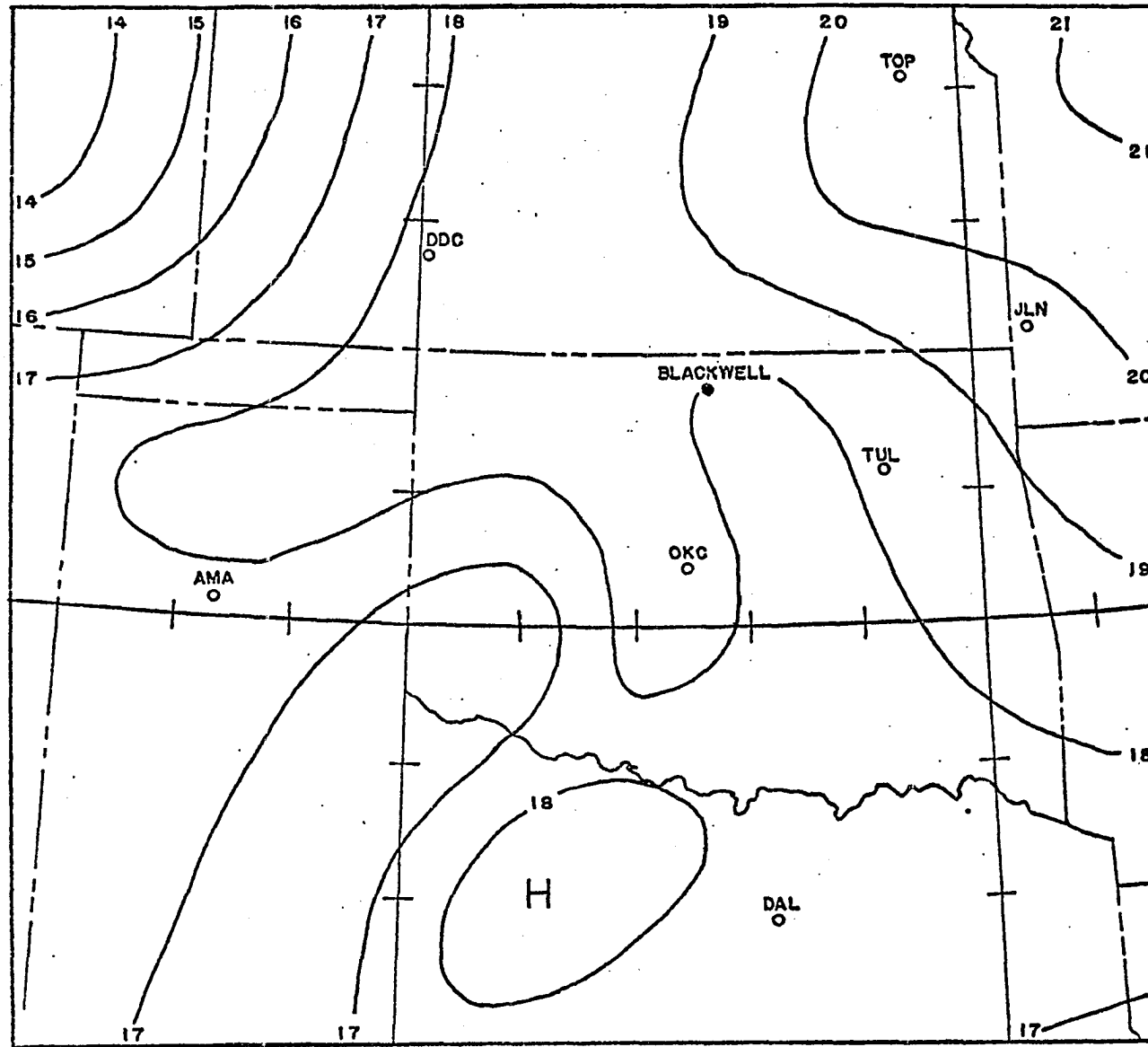


Fig. 7. Surface situation of 17/0700 CDT. The Oklahoma area is under the influence of a strong high centered over Lake Michigan. The morning stabilities were high due to subsidence and radiation cooling.

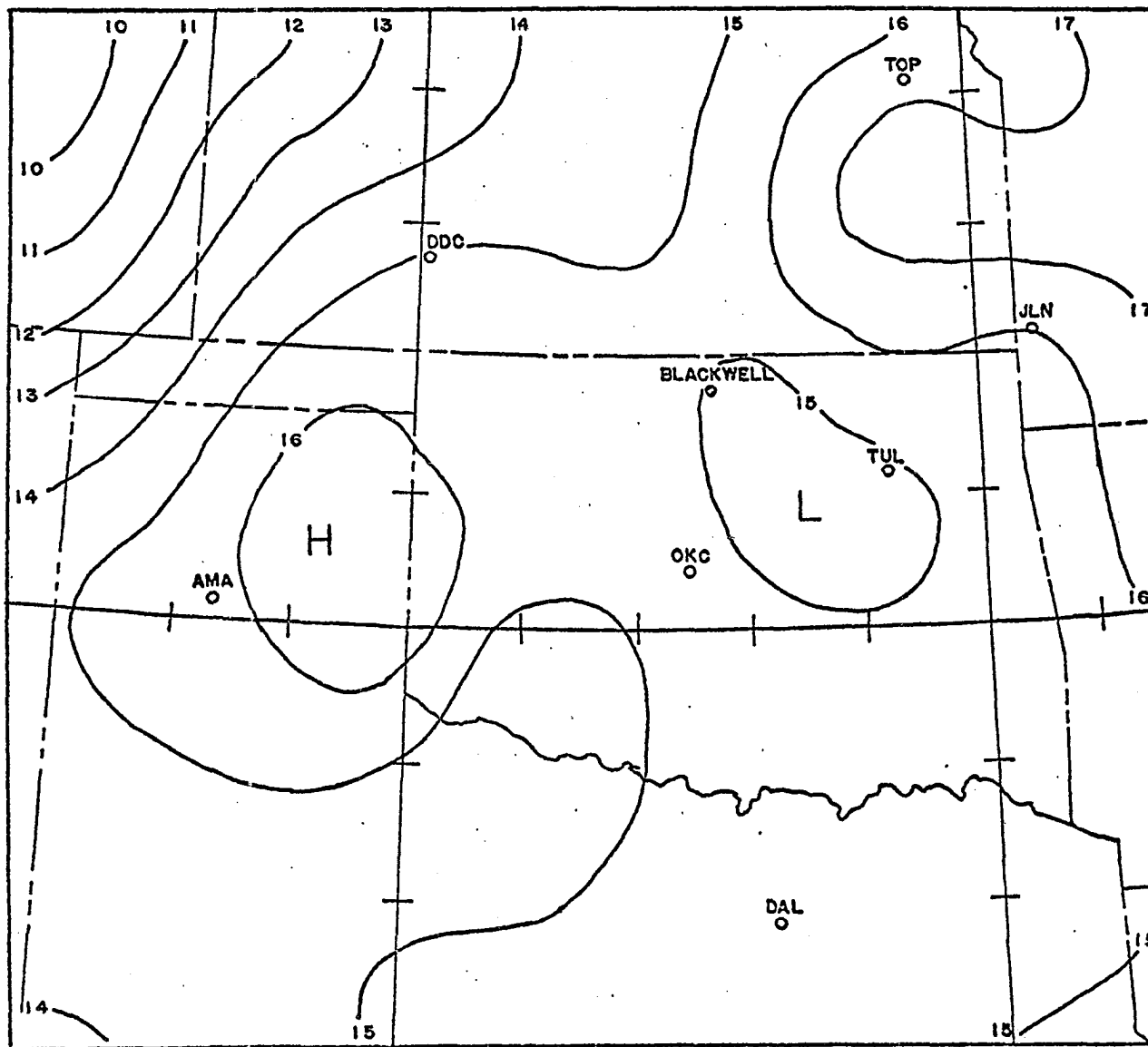


Fig. 8. Surface situation of 17/1900 CDT. In spite of the subsidence, there was enough heating to break the inversion in the afternoon.

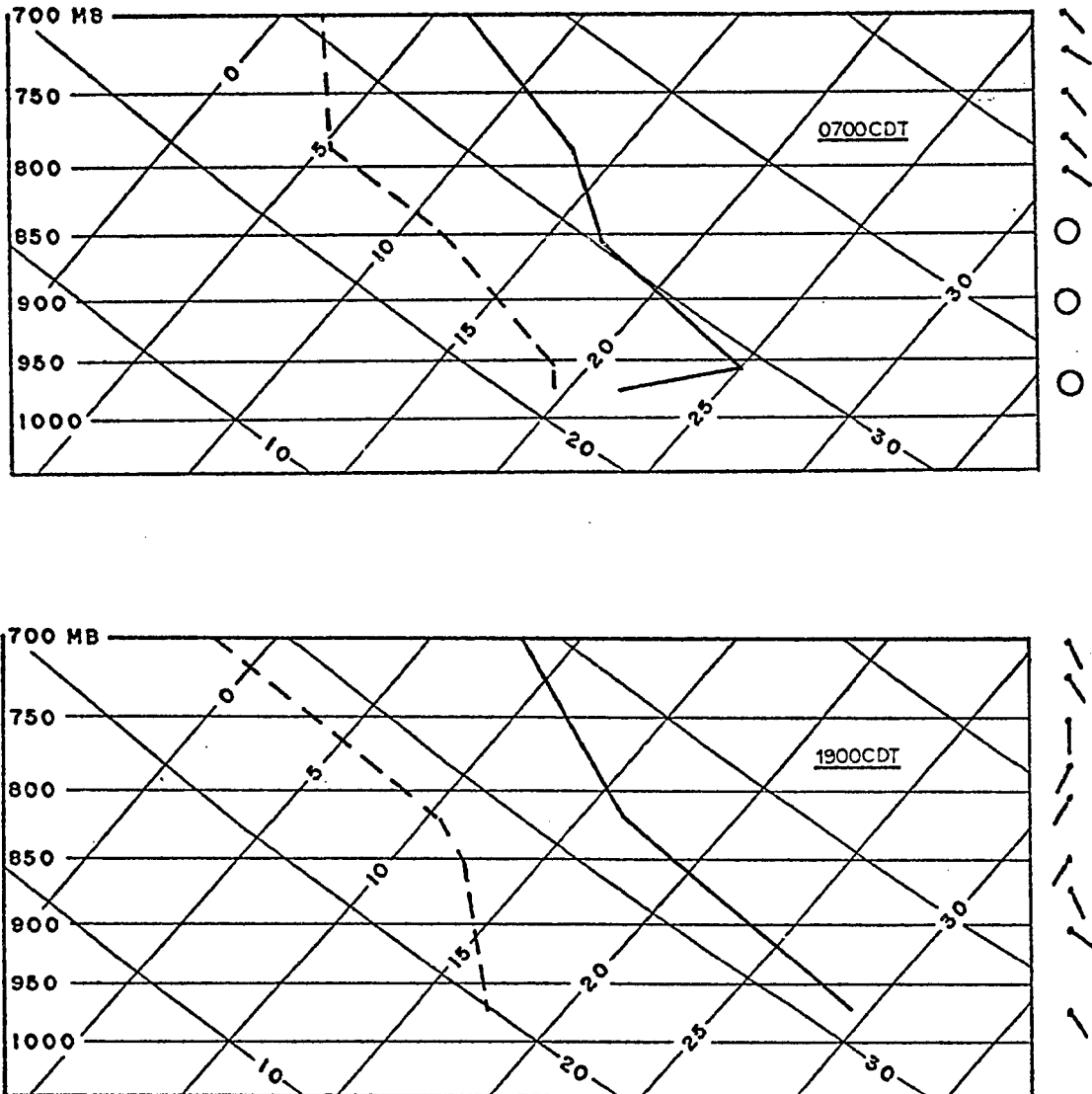


Fig. 9. The morning and afternoon soundings for Oklahoma City [TIK] of 17 August, 1971. Early in the morning there is an inversion due to subsidence and radiational cooling. During the day there was enough heating to break the inversion. The winds throughout the day remained light.

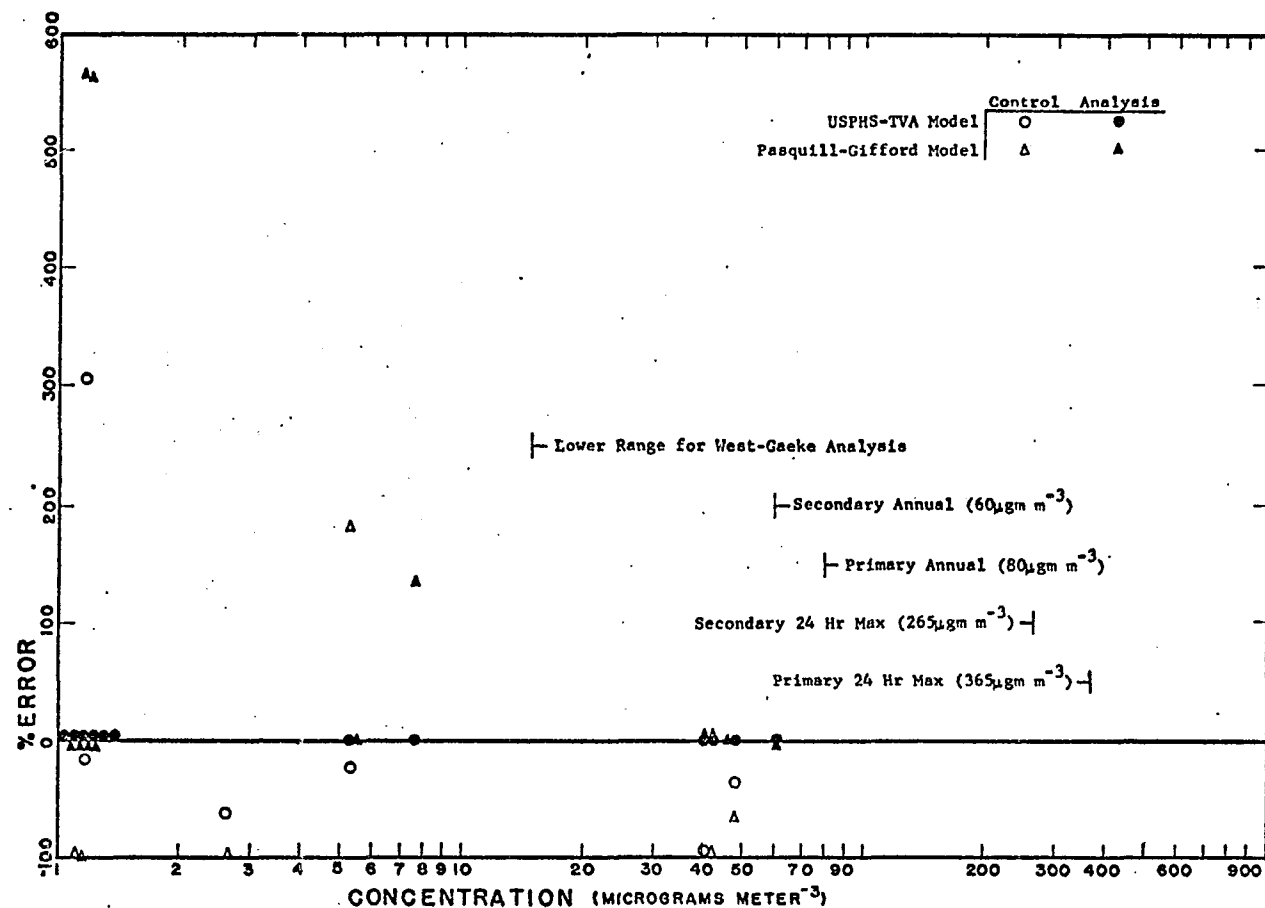


Fig. 10. Percent error versus sample size for runs of Tables II, III, and IV. Included are values of the national primary and secondary ambient standards. The best accuracy for both control data and reconstructed analysis data is for large concentrations. The West-Gaeke chemical analysis is valid in the range 15 to 293 $\mu\text{gm m}^{-3}$. In the background level (approx. $1 \mu\text{gm m}^{-3}$) only order of magnitude can be surmised.

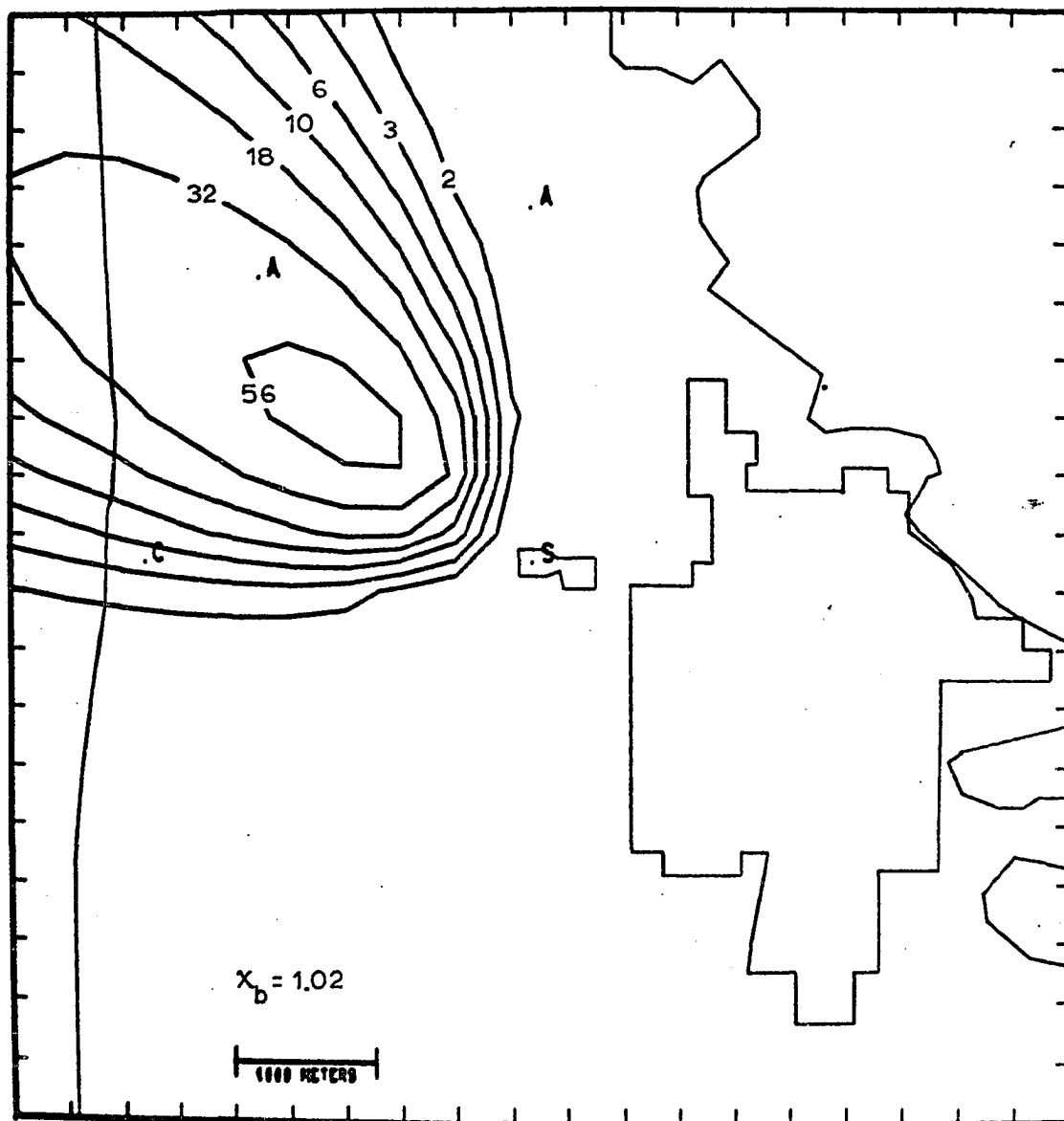


Fig. 11. Contoured values of contamination for the afternoon of the 17th. The USPHS-TVA model was used to estimate diffusion and the results are unfiltered. The analysis used two samples taken at roughly the same time and the optimal background contamination, χ_b , is 1.02 micrograms per cubic meter. In this and subsequent contoured figures, an 'A' indicates a site used in the analysis and a 'C' marks the location of a control sample. The location of a pseudo-source is indicated by an 'S'. Contoured units are in micrograms of sulfur dioxide per cubic meter.

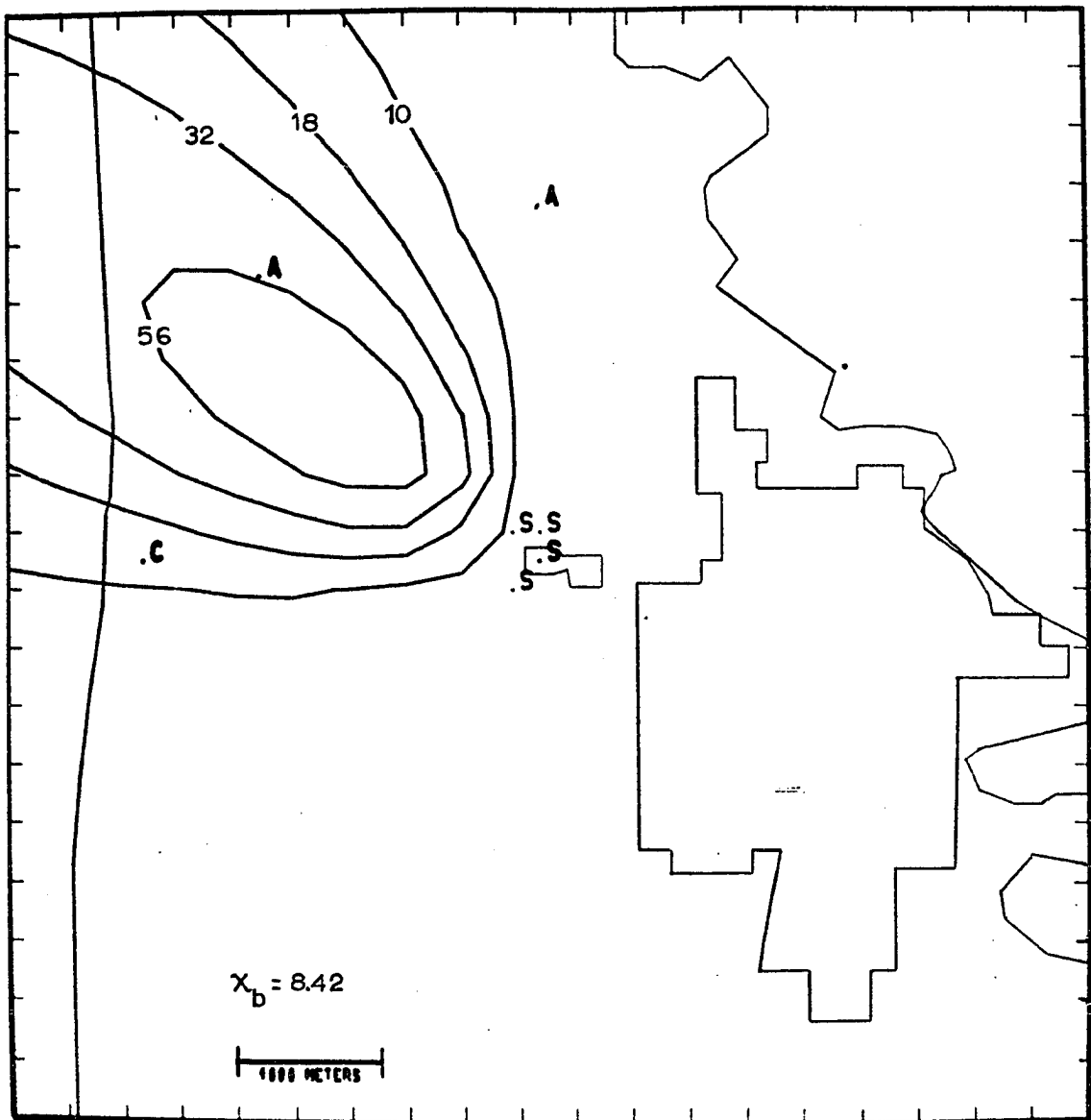


Fig. 12. Same as Fig. 11 except the analysis used samples taken throughout the working portion of the day. The same site was used as a control and a higher background, 8.42, resulted from the use of samples from different time periods.

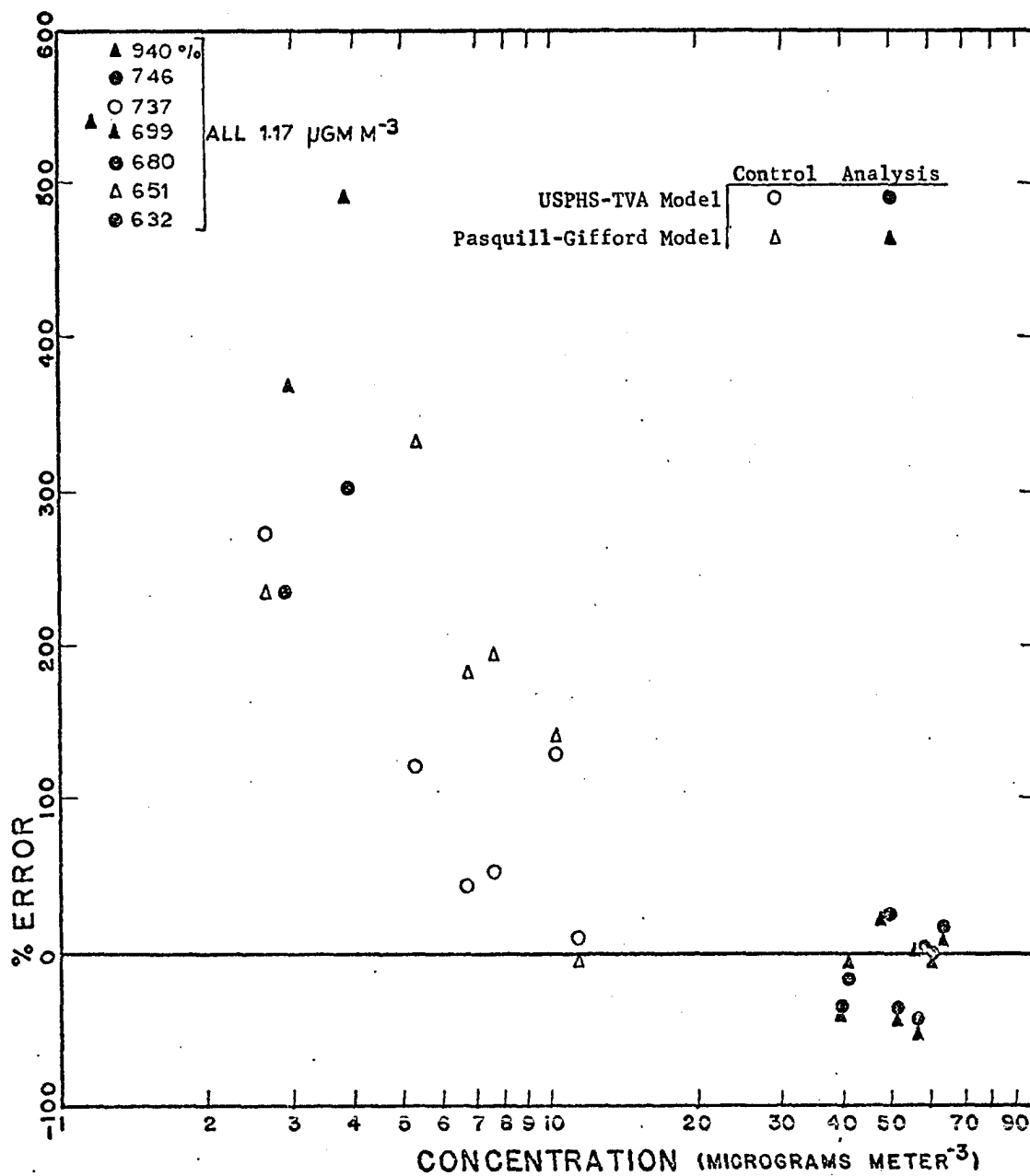


Fig. 13. Percent error versus concentration for runs represented by Tables V and VI.

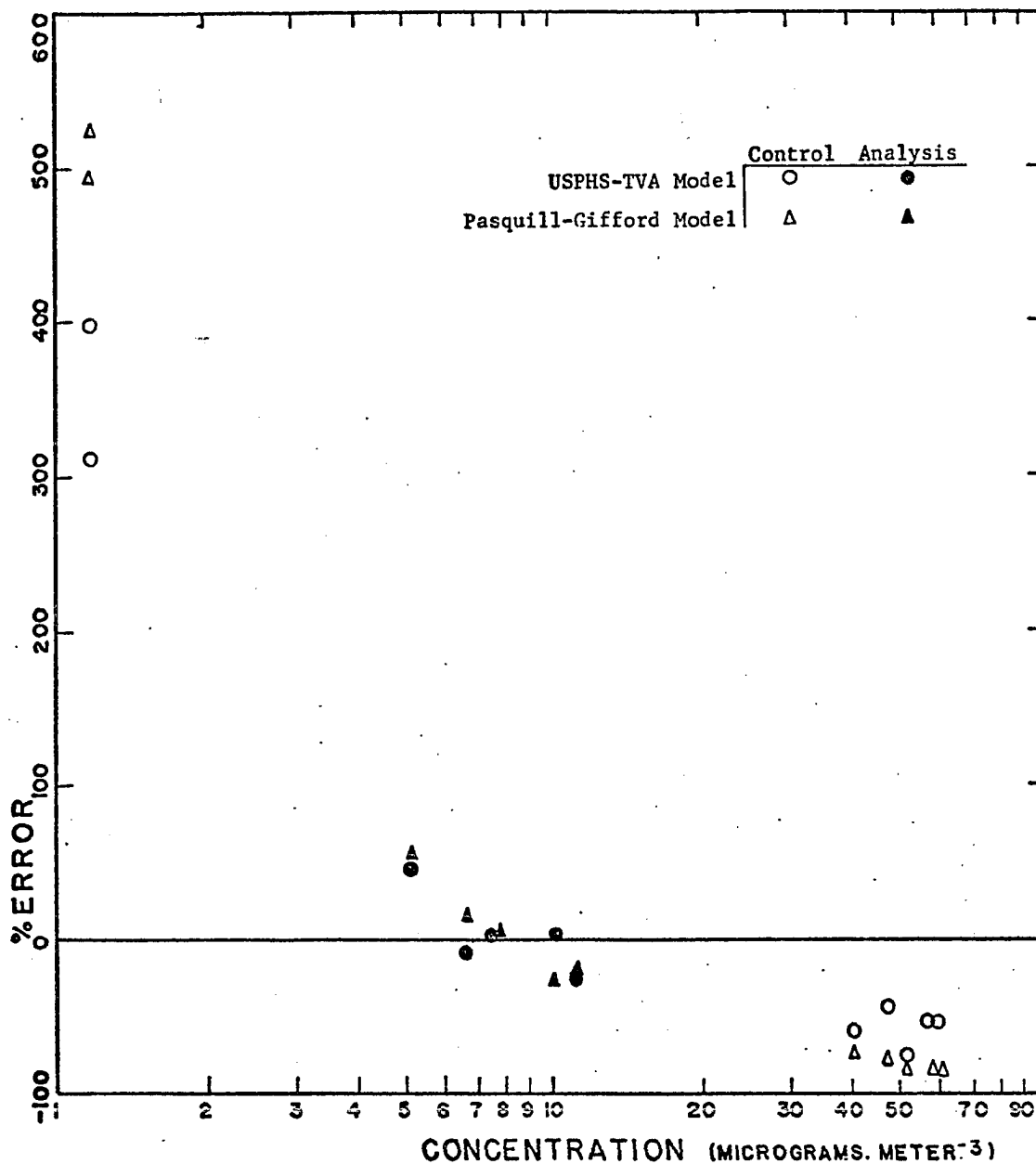


Fig. 14. Percent error versus sample size from multiple period analysis of working portion of the 17th. Two out of three sites were input as controls. The greatest error occurred for the small control samples.

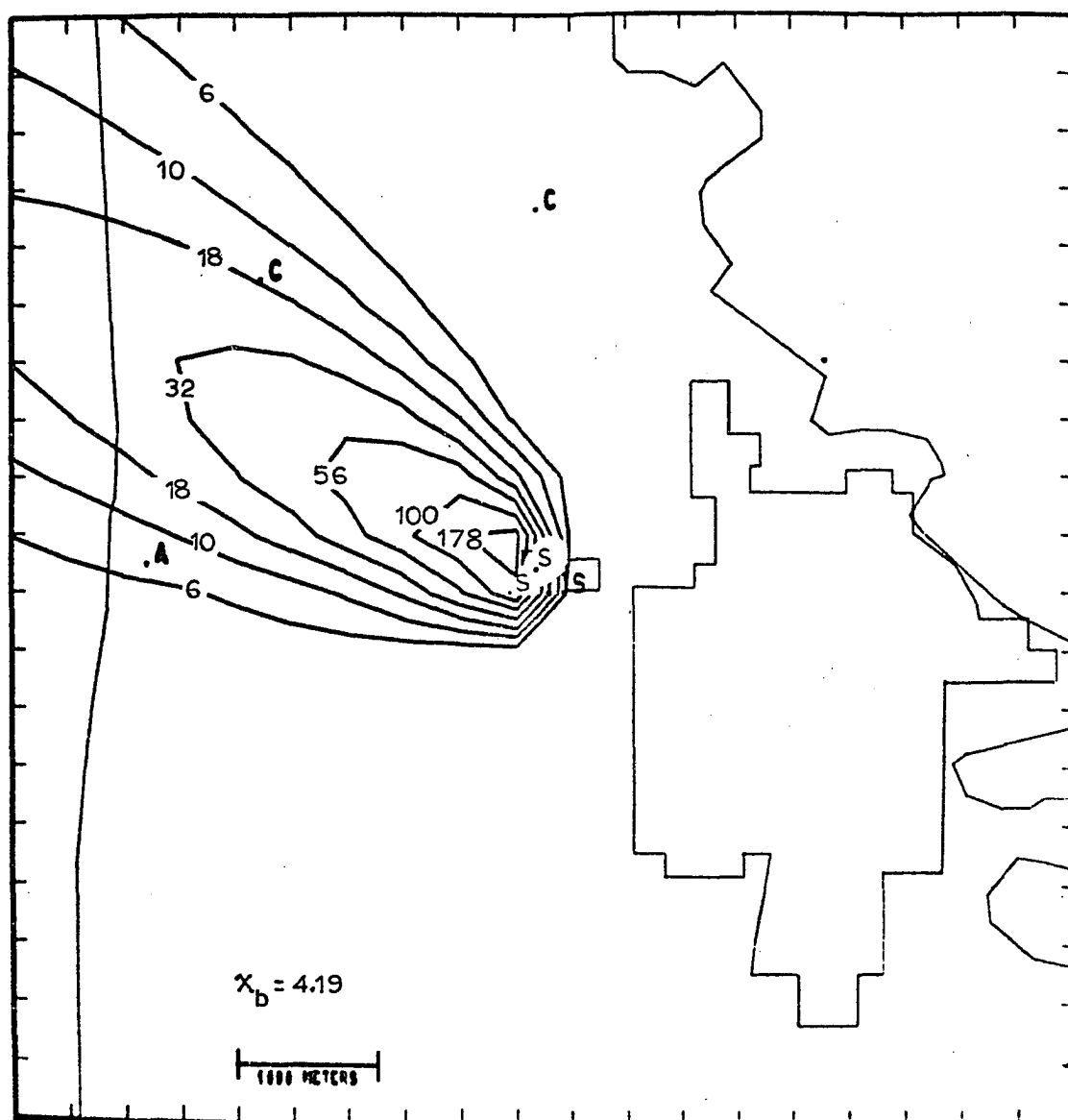


Fig. 15. Nonfiltered results from analysis of one sample site's data incorporating the working portion of the 17th. The USPHS-TVA model was used in this optimization analysis and the valid time of the contours is 0830 to 1000 CDT. The background contamination is 4.19.

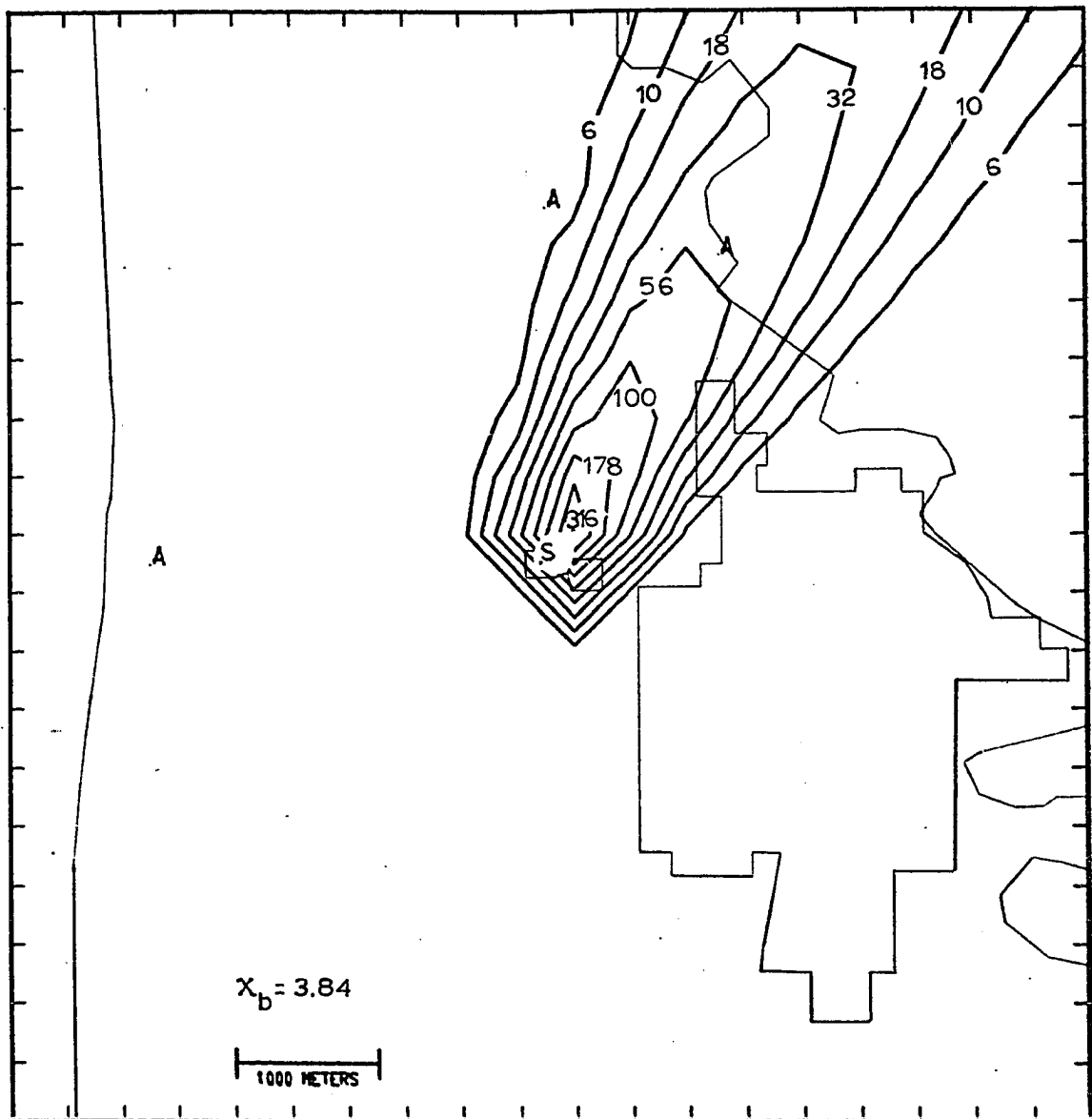


Fig. 16. Wednesday morning, 0800 - 1000 CDT, 11 August, 1971. This figure is the filtered result of using samples taken at roughly the same time (single period sampling) in the analysis. The background contamination is 3.84.

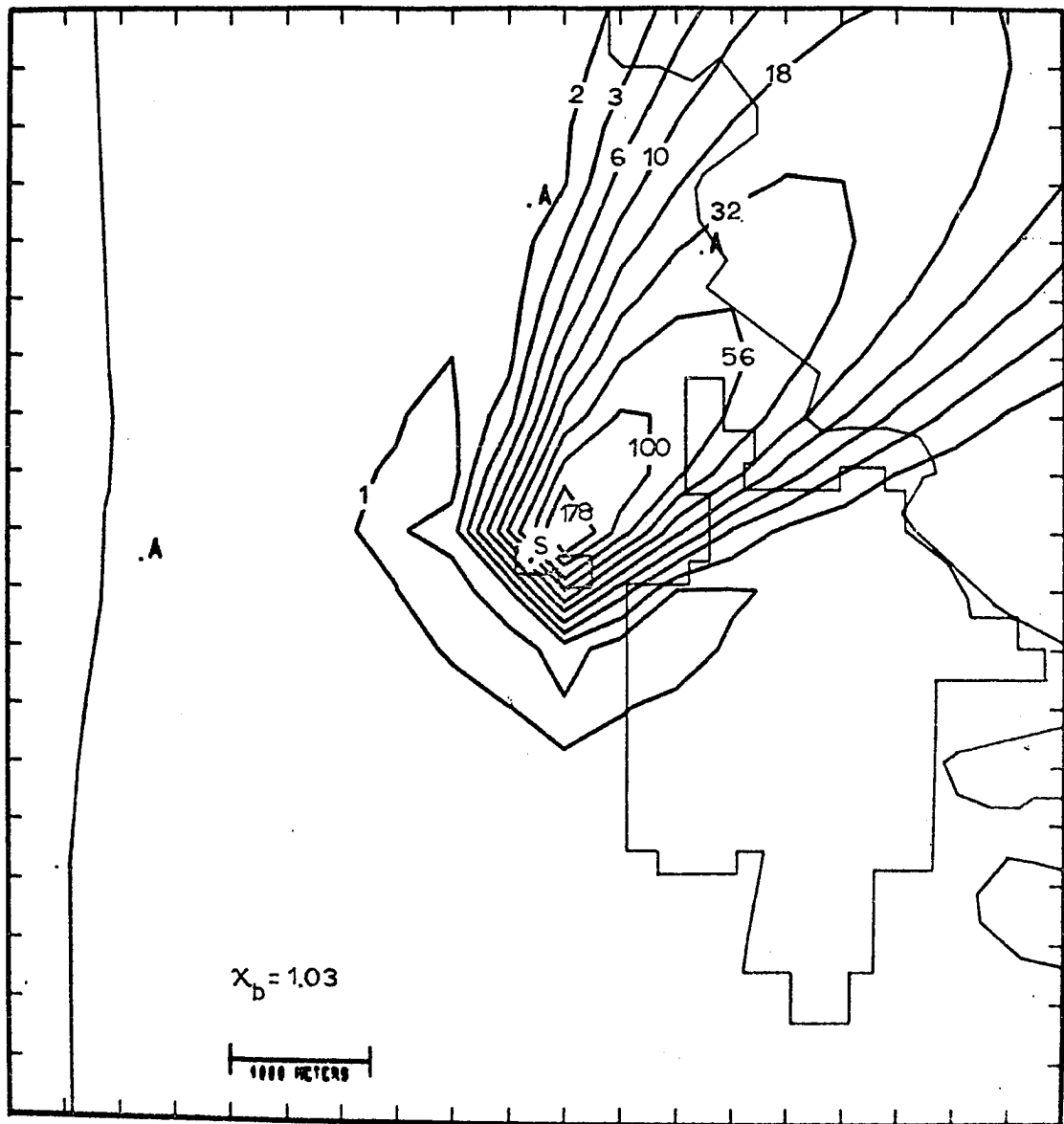


Fig. 17. Wednesday afternoon, 1400 - 1600 CDT, 11 August, 1971. The bent contour in the vicinity of the upper central data site is an example of the filtering scheme attempting to fit the analysis to input data. The crescent shaped area upwind to the smelter encloses an area with less than background contamination. This is an example of the low pass filter giving an erroneous solution in the vicinity of a strong first order discontinuity. The background contamination is 1.03. The rest is the same as Fig. 16.

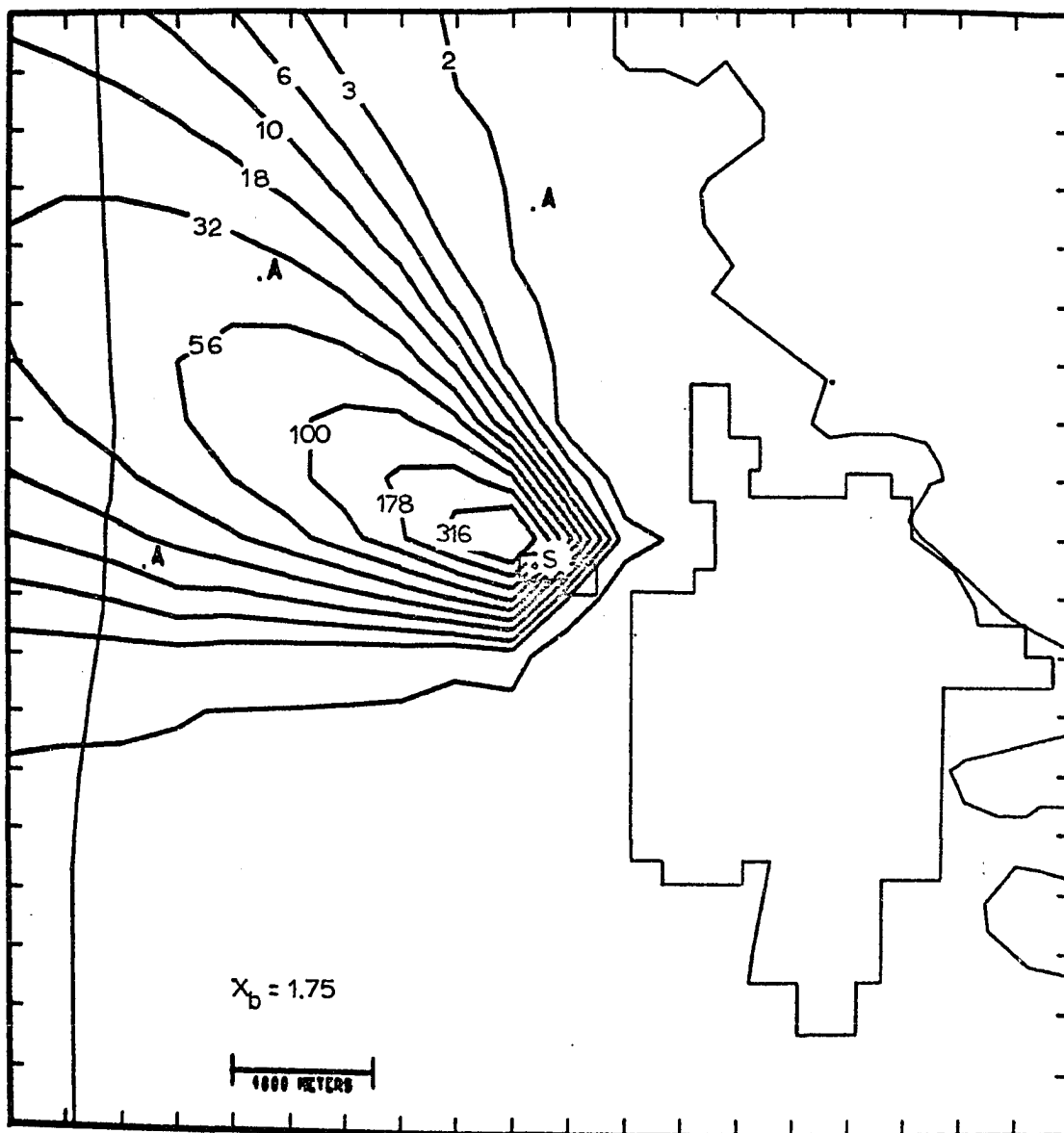


Fig. 18. Tuesday morning, 0815 - 1015 CDT, 17 August, 1971. Rest same as Fig. 16 except that the Pasquill-Gifford model was used in the analysis. The background contamination is 1.75.

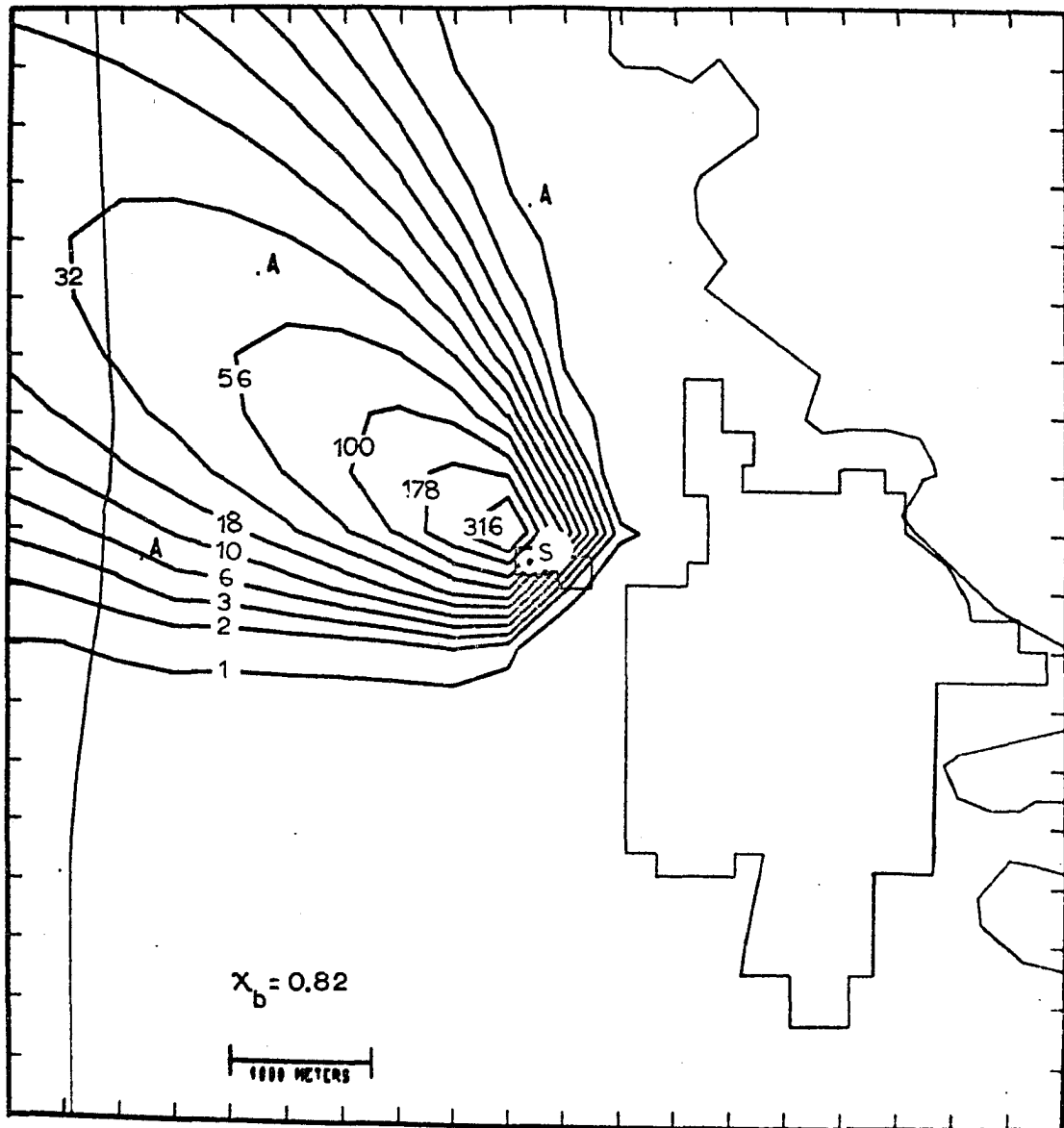


Fig. 19. Tuesday afternoon, 1615 - 1815 CDT, 17 August, 1971. The background contamination is 0.82. The rest is the same as Fig. 16.

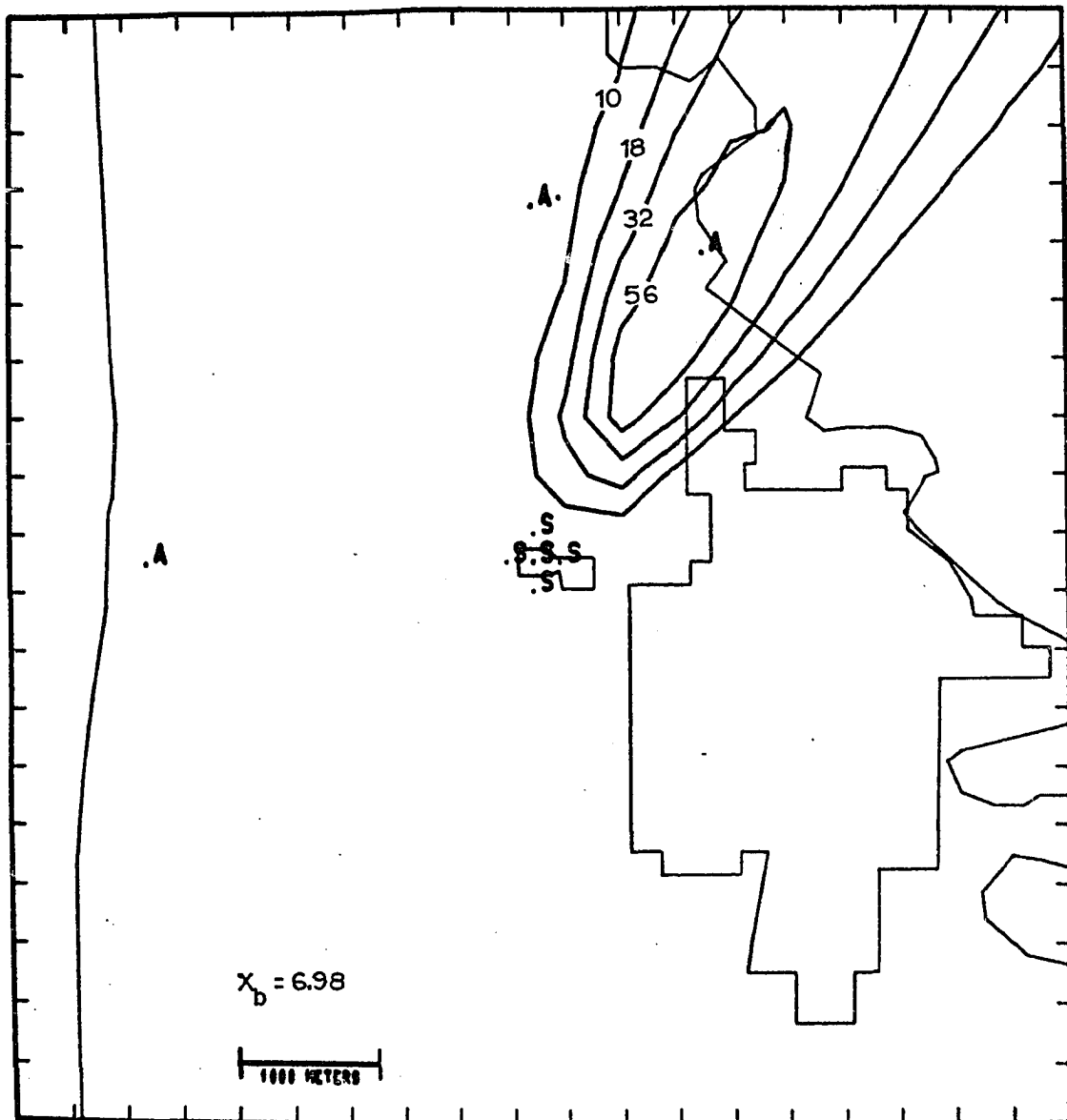


Fig. 20. Wednesday morning, 0800 - 1000 CDT, 11 August, 1971. This figure is the filtered result of applying the optimized parameters found using all the pollution data from the complete working day (multiple period sampling). The background contamination is 6.98.

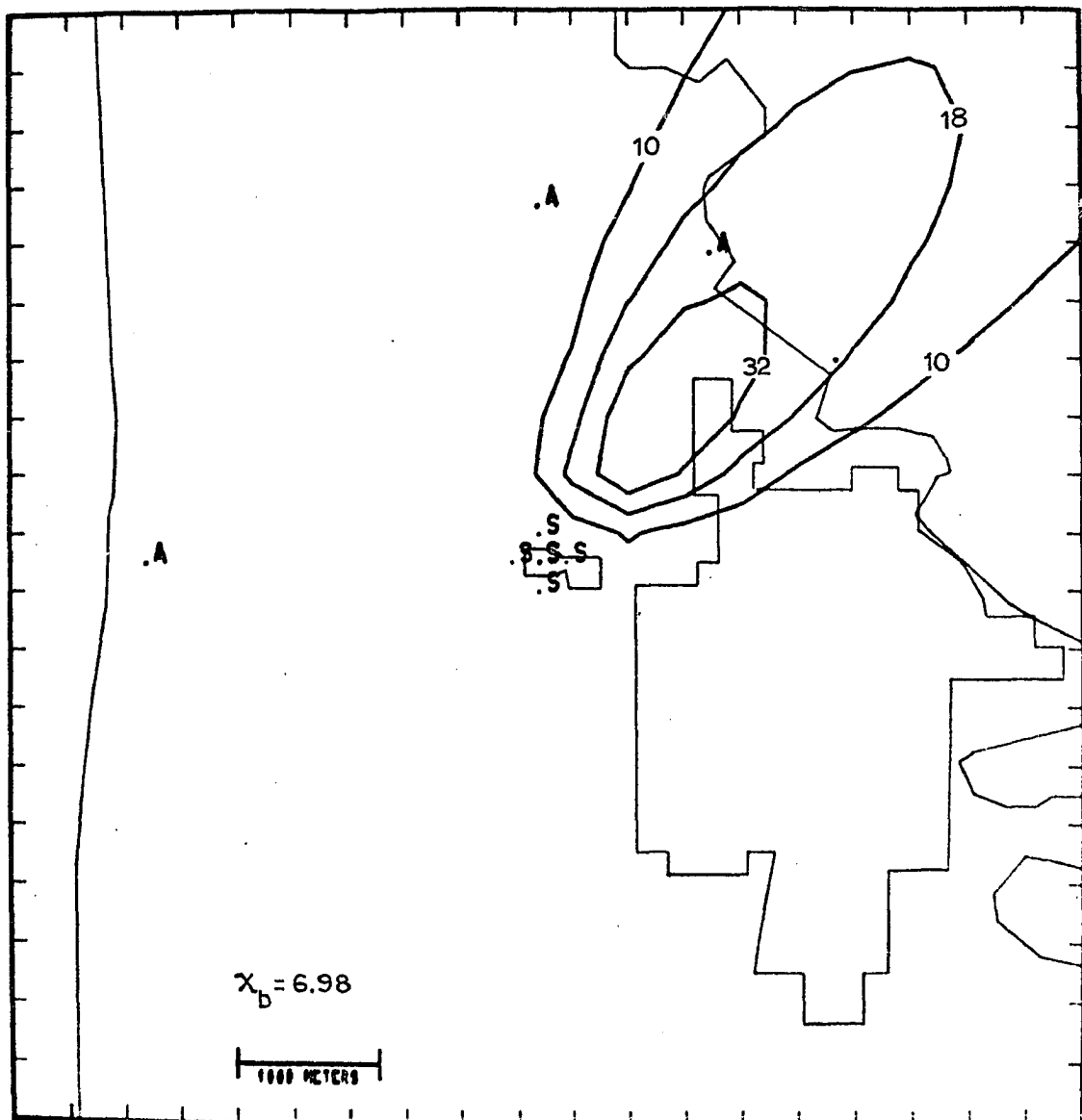


Fig. 21. Wednesday afternoon, 1400 - 1600 CDT, 11 August, 1971. The background contamination is 6.98. The rest is the same as Fig. 20.

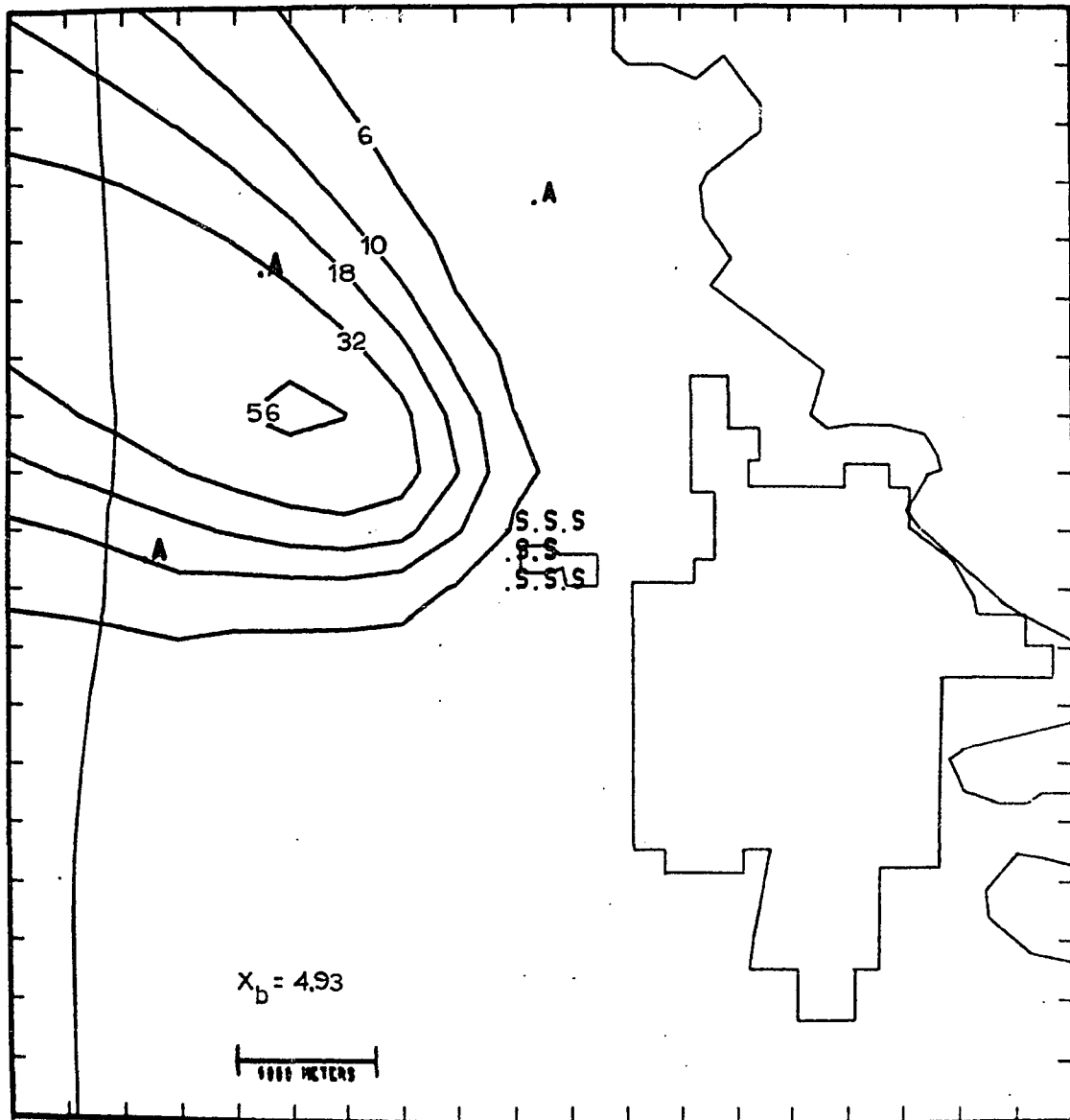


Fig. 22. Tuesday morning, 0815 - 1015 CDT, 17 August, 1971. The background contamination is 4.93. The rest is the same as Fig. 20.

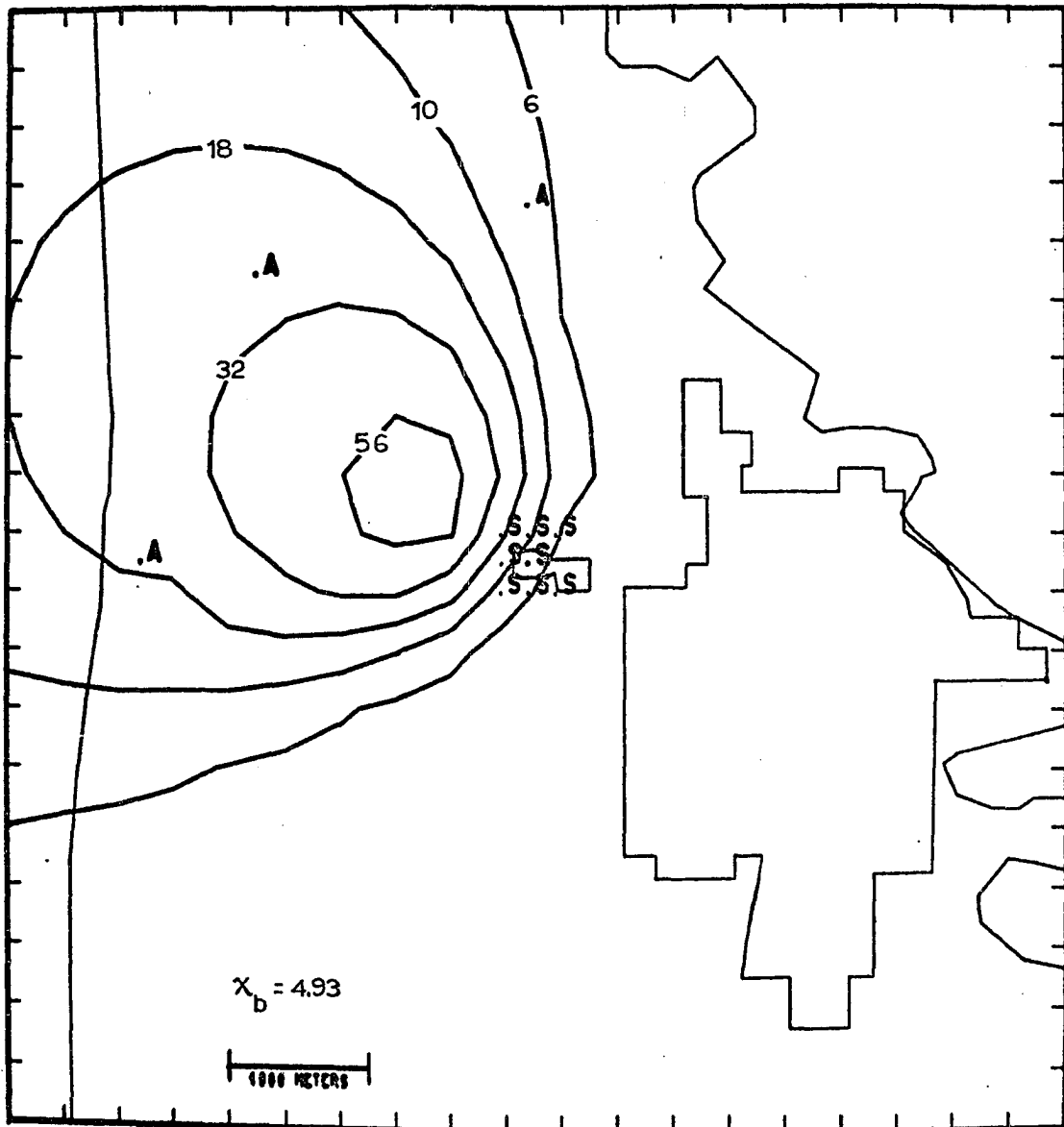


Fig. 23. Tuesday afternoon, 1415 - 1615, CDT, 17 August, 1971. The background contamination is 4.93. The rest is the same as Fig. 20.